Temporally Evolving Gain Mechanisms of Attention in Macaque Area V4

4 authors, including:

Ilaria Sani
The Rockefeller University
5 PUBLICATIONS **65** CITATIONS

SEE PROFILE

Leonardo Chelazzi
University of Verona
97 PUBLICATIONS **7,585** CITATIONS

SEE PROFILE

Some of the authors of this publication are also working on these related projects:

Project Distractor Suppression View project

Project Attention & Contrast - revisited View project

RESEARCH ARTICLE | *Higher Neural Functions and Behavior*

Temporally evolving gain mechanisms of attention in macaque area V4

Ilaria Sani,[1,2] ● **Elisa Santandrea,**[1] ● **Maria Concetta Morrone,**[3,4] **and** ● **Leonardo Chelazzi**[1,5]

[1]*Department of Neuroscience, Biomedicine and Movement Sciences, University of Verona, Italy;* [2]*The Rockefeller University, New York, New York;* [3]*Department of Translational Research on New Technologies in Medicine and Surgery, University of Pisa, Italy;* [4]*Stella Maris Foundation, Pisa, Italy; and* [5]*National Institute of Neuroscience, Verona, Italy*

Sani I, Santandrea E, Morrone MC, Chelazzi L. Temporally evolving gain mechanisms of attention in macaque area V4. *J Neurophysiol* 118: 964–985, 2017. First published May 3, 2017; doi: 10.1152/jn.00522.2016.—Cognitive attention and perceptual saliency jointly govern our interaction with the environment. Yet, we still lack a universally accepted account of the interplay between attention and luminance contrast, a fundamental dimension of saliency. We measured the attentional modulation of V4 neurons' contrast response functions (CRFs) in awake, behaving macaque monkeys and applied a new approach that emphasizes the temporal dynamics of cell responses. We found that attention modulates CRFs via different gain mechanisms during subsequent epochs of visually driven activity: an early contrast-gain, strongly dependent on prestimulus activity changes (baseline shift); a time-limited stimulus-dependent multiplicative modulation, reaching its maximal expression around 150 ms after stimulus onset; and a late resurgence of contrast-gain modulation. Attention produced comparable time-dependent attentional gain changes on cells heterogeneously coding contrast, supporting the notion that the same circuits mediate attention mechanisms in V4 regardless of the form of contrast selectivity expressed by the given neuron. Surprisingly, attention was also sometimes capable of inducing radical transformations in the shape of CRFs. These findings offer important insights into the mechanisms that underlie contrast coding and attention in primate visual cortex and a new perspective on their interplay, one in which time becomes a fundamental factor.

NEW & NOTEWORTHY We offer an innovative perspective on the interplay between attention and luminance contrast in macaque area V4, one in which time becomes a fundamental factor. We place emphasis on the temporal dynamics of attentional effects, pioneering the notion that attention modulates contrast response functions of V4 neurons via the sequential engagement of distinct gain mechanisms. These findings advance understanding of attentional influences on visual processing and help reconcile divergent results in the literature.

contrast response functions; gain mechanisms of attention; macaque area V4; spatial attention; temporal dynamics

INFORMATION PROCESSING along the visual hierarchy reflects not only the physical properties of the image but also the goals of the observer, which decree the relevance of specific items. Spatial attention supports enhanced analysis at specific spatial locations deemed of potential interest for behavior. In the last decades, several studies examined the interplay between spatial attention and luminance contrast, a key physical property of the visual input, in determining neuronal activity in cortical visual areas. Multiple models have been proposed to account for the effects of attention on contrast response functions (CRFs), including contrast gain (Martínez-Trujillo and Treue 2002; Reynolds et al. 2000), multiplicative rescaling (Williford and Maunsell 2006), and additive models (Thiele et al. 2009). A unifying normalization model of attention (Lee and Maunsell 2009; Reynolds and Heeger 2009) attempted to reconcile such divergent results, suggesting that different gain modulations may all derive from a common circuit when probed under different conditions.

In the present article we describe a novel approach to investigate the impact of attention on CRFs in macaque area V4, hinging on a detailed analysis of the temporal dynamics of CRFs, and of their modulation by attention. Time is a critical factor in visual processing. To begin with, visual responses are dynamic in nature, being characterized by transient and sustained components (e.g., Albrecht et al. 1984). Even more interestingly, time is crucial in relation to a wide range of phenomena that have been demonstrated to develop dynamically. For example, selectivity for basic visual features has been shown to build up and refine over time (Ringach et al. 1997; Shapley et al. 2003). We recently demonstrated that selectivity for contrast in macaque area V4 emerges slowly as a result of a time-consuming recurrent process, likely implementing gradually stronger inhibition of responses to high contrasts via a normalization mechanism (Sani et al. 2013). Time is also crucial for the expression of more complex forms of selectivity, as involved in figure-ground segmentation, and in relation to context-sensitive phenomena reflecting the global interpretation of a visual scene (Jeurissen et al. 2013; Kogo and Wagemans 2013). A further example is the delayed emergence of border-ownership signals in V2 (and V4) cells (Sugihara et al. 2011; Zhou et al. 2000). Yet other forms of selective coding of relevant information in cortical visual areas, such as the categorical representation of attended features at the service of behavior, show a strongly delayed emergence in V4 (Mirabella et al. 2007). A distinct temporal dynamics also characterizes surround suppression mechanisms, arising from the basic center-surround organization of inputs to visual neurons: while the excitation from the receptive field (RF) is short latency and transient, the suppressive signal from the surround exerts a delayed and prolonged effect on neuronal activity (Bair et al. 2003; Henry et al. 2013). In all cases, a fine analysis of the temporal unfolding of these phenomena enabled important

Address for reprint requests and other correspondence: L. Chelazzi, Dept. of Neuroscience, Biomedicine and Movement Sciences, Section of Physiology and Psychology, Univ. of Verona, Strada Le Grazie 8, 37134 Verona, Italy (e-mail: leonardo.chelazzi@univr.it).

observations concerning the underlying neurobiological, circuit-level mechanisms, especially in relation to the contribution of intra- vs. inter-area communication (e.g., Layton et al. 2012).

Despite hints in the literature suggesting that attentional modulation can be particularly evident in critical time epochs (Buffalo et al. 2010; Fries et al. 2008; Hayden and Gallant 2005; Lee et al. 2007; McAdams and Maunsell 1999; Reynolds et al. 2000) and recent computational work underscoring the theoretical importance of including time dependency in the framework of the normalization model of attention (Smith et al. 2015), a fine temporal characterization of the interplay between contrast and attention in visual cortex is still lacking.

We designed a paradigm with macaque monkeys where attention was to be covertly deployed toward a stimulus either inside or outside the RF of the recorded neuron, and the stimuli, unpredictable in time and contrast value, were maintained until the behavioral decision was made. This allowed us to investigate the temporally evolving interaction between varying stimulus contrast and spatial attention in determining neuronal responses in macaque area V4. In addition, we took into proper consideration heterogeneous contrast coding in macaque area V4 (Sani et al. 2013; see also Peirce 2007). As a result, diverse attentional gain mechanisms emerged along subsequent phases of visual processing. Importantly, attention to the RF modulated similarly cells showing different contrast coding properties (Sani et al. 2013), which indicates that general mechanisms are involved. Finally, attention was sometimes capable of inducing radical changes in the shape of neuronal CRFs, suggesting that contrast coding is not a rigid property of the given neuron.

We chose a paradigm wherein the monkeys were informed in advance of the behaviorally relevant location, an approach that previously allowed measurement of anticipatory attentional effects on baseline activity (the so-called "baseline shift"; Buffalo et al. 2010; Luck et al. 1997; McAdams and Maunsell 1999; Reynolds et al. 2000). Despite a rich literature, it is not completely clear whether feedback from high-level areas of the attentional network to visual cortex begins before the critical stimulus appears or is triggered by the onset of the stimulus, nor how prestimulus and stimulus-evoked attentional modulation interact to determine modulation of neuronal firing over time (see Sylvester et al. 2009 for a review of relevant literature). On the one hand, the baseline shift and the poststimulus attentional modulation might reflect completely independent processes. On the other hand, a unique attentional signal might be responsible for enhancing neuronal activity both before and after the onset of a visual stimulation (Buracas and Boynton 2007; Sylvester et al. 2009). Our results contribute to the understanding of this complex scenario; specifically, we demonstrate that the attentional modulation in the poststimulus epoch reflects diverse gain mechanisms and that these gain mechanisms depend to a differing degree on the prestimulus effect.

At a general level, our findings help reconcile previous reports on the interplay between attention and luminance contrast in area V4, which sometimes yielded divergent results, and bring new evidence in favor of the proposed unifying role of V4 to enable extraction of functional networks both by bottom-up and top-down attentionally driven selection (Roe et al. 2012).

MATERIALS AND METHODS

Experiments were performed on two head-fixed, nonanesthetized male adult macaque monkeys (*Macaca mulatta*; *monkeys F* and *T*) weighing 10 and 8 kg, respectively. Experiments were performed in accordance with national laws on care and use of laboratory animals and with the European Community Council Directive of September 22, 2010 (2010/63/EU). All experimental protocols were approved by the University of Verona Committee for Animal Research (CIRSAL) and by the Department for the Veterinary Public Health, Nutrition and Food Security of the Italian Ministry of Health (D.L. n. 116/1992, art. 8/9; D.M. n. 19/2007c, 13/02/2007, and n. 200/2009c, 11/11/2009).

Behavioral paradigm. We trained the animals to discriminate the orientation of achromatic bar stimuli in return for juice reward. Each trial began with the presentation of a fixation point (black square, $0.3° \times 0.3°$ of visual angle; Fig. 1A) on a dark background (2.49 cd/m^2). Monkeys were required to hold fixation for the entire duration of the trial; eye position was continuously monitored with the eye-coil technique (1 kHz) such that if at any time during the trial the eyes deviated more than 1° from the fixation point, the trial was aborted and no reward was delivered. After the animal acquired fixation, a pentagon or a triangle cue ($1.3° \times 1.3°$, 20% Michelson contrast) was presented at the center of gaze, which instructed the monkey to covertly direct attention to a position respectively outside or inside the RF of the neuron under study. After a delay, which varied between 800 and 1200 ms, two bars ($2.2° \times 0.3°$) were simultaneously presented, one inside and one outside the RF, and they were placed in symmetrical positions with respect to the fixation spot and at equal distance from it. The bars were shown at either of two possible orientations (the optimal and one suboptimal for the recorded neuron); combinations of the stimulus orientations presented at the two locations on the screen were controlled to ensure an equal number of congruent vs. incongruent conditions, i.e., conditions in which the two orientations required the same or a different behavioral response, respectively. To earn a juice reward, the monkey had to discriminate the orientation of the bar at the cued location (while ignoring the bar at the opposite location) by turning a lever in the appropriate direction, based on stable, previously learned stimulus-response associations (e.g., during the training phase, the animal learned to turn the lever to the right in response to a vertical bar and to a −45° tilted bar, and to turn the lever to the left in response to a horizontal bar and to a +45° tilted bar; note that two orientations requiring opposite responses were selected for each recording session; see above). Congruent and incongruent conditions were important to ensure that the animal was correctly paying attention to the cued location; performance in both conditions was always above 70% correct (see below). The bar inside the RF was displayed at any of seven or nine (for different cells) positive contrast levels (from 2.5 to 94% Michelson contrast) selected randomly on each trial; additionally, on some trials a virtual, zero-contrast bar (null stimulus) was displayed inside the RF, and the monkey was rewarded for any response. The contrast of the stimuli was task irrelevant, although it contributed significantly to the discriminability of target stimuli. The bar outside the RF was of constant contrast (20%) for one animal (*monkey F*), whereas it varied between 10% and 80% Michelson contrast for the other animal (*monkey T*); in the latter case, contrast at the two locations was independently selected on a random basis. We adopted such protocol for the second animal to have the animal perform a nearly identical, unbiased task in the two attentional conditions. Importantly, we could detect no appreciable difference between the two monkeys in terms of behavioral performance or neuronal responses (see RESULTS). For each recorded neuron, the two attentional conditions were organized in independent alternating blocks of trials; multiple alternations between block types ensured that any differences across attentional conditions could not be the result of even small changes in neuronal excitability along the session. Several features of the task were aimed at keeping the animal's attention as constant as possible across trials and conditions.
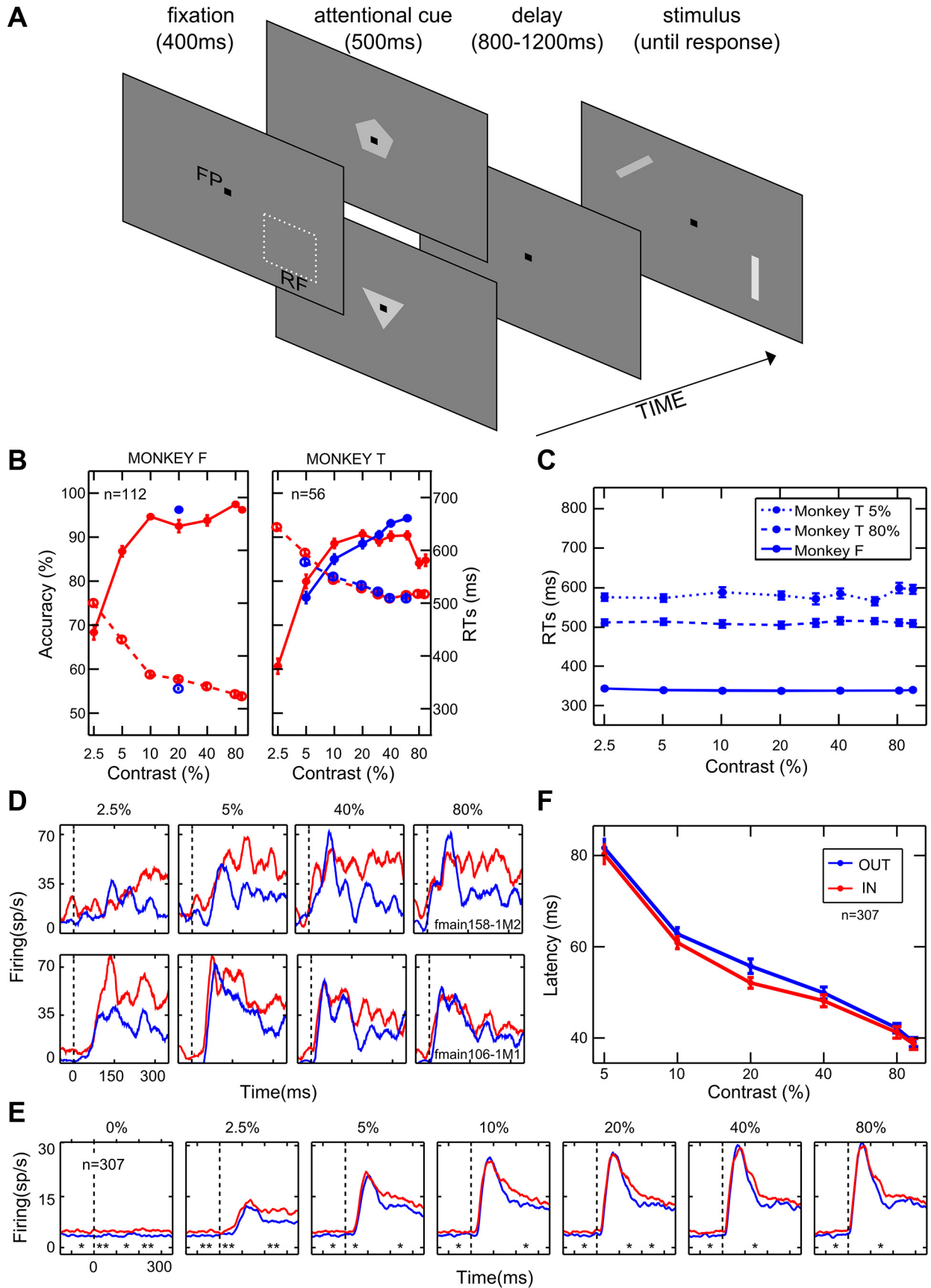
First, the use of random target onset times encouraged the animals to maintain constant vigilance and sustained attention at the cued location. Second, the use of the same task at the two locations ensured that the effects of directed attention were not contaminated by any influence of a different level of alertness. Third, the presence of a distracter on all trials ensured a constant effort across trials. Note, however, that the presence of a distracter might also result in a potentially nontrivial problem; i.e., it might cause unwanted shifts of attention in space depending on the relative saliency between the two stimuli on the display. Although we were confident that stable allocation of spatial attention was obtained as the result of extensive training, we directly assessed the influence of the distracter contrast on attentional allocation by verifying its impact on the animals' behavior (see RESULTS). In case the animal's attention was automatically attracted by a (high contrast) distracter and had to return to the (low contrast) target for allowing correct performance, we would expect a slowing of reaction times (RTs) in that condition, which was not the case in our data (see RESULTS).

Surgical procedures and electrophysiological recordings. Surgical procedures and recording methods are described in detail elsewhere (Mirabella et al. 2007; Sani et al. 2013). In brief, after the animals were trained on the behavioral task, a recording chamber was implanted over V4 in each animal, based on MRI-guided brain reconstruction. Recordings were made using tungsten microelectrodes (1 MΩ); extracellular signals were filtered and amplified. Action potentials from individual neurons were discriminated using an online spike-sorting system and digitized for offline analysis at 1 kHz on a personal computer. In most cases, two (up to 4) neurons could be recorded simultaneously and accurately differentiated on the basis of the size and shape of the spike waveform.

During electrophysiological recordings, before the behavioral experiment was commenced, with the use of a hand-controlled visual stimulus, each well-isolated cell was carefully characterized to determine the RF location and preference for orientation (and sometimes for other stimulus properties, such as color and spatial frequency), as well as its response to contrast, while the monkey fixated centrally. The RF size was estimated using the minimum response field method (Barlow et al. 1967). Bar stimuli of a fixed size ($2.2° \times 0.3°$; see below) were used throughout to be well within the classical RF boundary of the recorded neurons, in accordance with data in the literature (Motter 2009) and as confirmed for each neuron during the initial mapping procedure by using flashing bars of different contrast levels, including high contrasts.

Recorded neurons were included in the analysis if *1*) at least 12 repetitions for each experimental condition were collected (with correct performance), *2*) recording quality was high and stable throughout the session, *3*) neurons were significantly responsive to at least one contrast level, and *4*) the animal's level of accuracy at the task was higher than 70% within the session for each experimental condition, including all contrast levels (except 2.5% contrast; see below) and attentional conditions, and with separate testing for congruent vs. incongruent trials, to ensure that attention was correctly

allocated to the cued spatial position in all trial types. Note that an accuracy >70% was not required for 2.5% contrast, which was selected to be close to the visibility threshold, because in this case poor performance would likely reflect perceptual difficulty rather than an improper allocation of attention.

Data analysis. Latency of the neuronal response was calculated separately for each contrast level and each attentional condition, using the method described by Gawne et al. (1996). Operationally, we constructed a PSTH and smoothed it with a Gaussian filter ($\alpha = 8$ ms); we then defined and calculated response latency as time to half the peak of the response waveform.

For each neuron, firing rates were determined by taking the average firing during a period of interest across all stimulus repetitions of the same experimental condition. In all cases, we considered time windows in the poststimulus phase (up to 300 ms), which ended before the behavioral response of the animal; thus in all cases we analyzed neuronal firing in epochs when the stimulus was stably present on the display. Given the relatively short RTs measured for one animal (*monkey F*), especially for responses to high-contrast stimuli (see RESULTS), we detected a few single trials (4 over >66,000) that did not match this requirement (i.e., in those trials the behavioral response was delivered with an RT <300 ms) and were therefore discarded. All the analyses were performed using stimulus-locked time windows, where neural activity was aligned to stimulus onset, and using response-locked (latency corrected) time windows, where neural activity was aligned to neuronal response latency (*time 0* in this version of the analysis), calculated as previously indicated.

For fine-grain temporal analyses we calculated mean firing rate in overlapping time windows (width 20 ms, shift 1 ms). To check for statistical significance of firing differences measured between attentional conditions within these fine-grained analyses, we applied non-parametric, trial-based random permutation tests (Astrand et al. 2015; Ibos et al. 2013). For each cell, we randomly reassigned the attended and unattended trials, and calculated the spike difference for each time window and contrast. The permutation procedure was performed 10,000 times to generate a distribution of 10,000 spike difference values against which the real difference was tested. The observed spike difference between attentional conditions was considered to be significant if it fell within the upper 5% of the permuted difference distribution. Results were confirmed by calculating a *P* value for the observed difference as follows: P = no. of spike differences resulting from the permutation procedure ≥ observed spike difference/10,000.

To characterize attentional effects within relevant time periods, three 90-ms-wide consecutive windows were used, i.e., an early window (30–120 ms), an intermediate window (120–210 ms), and a late window (210–300 ms), time-locked to the stimulus onset. In the latency-corrected condition, these windows were set to be 80 ms wide, starting from response onset (0–80 ms, 80–160 ms, 160–240 ms). In both cases, windows and their duration were chosen on the basis of the temporal dynamics of attentional effects at the population level (see RESULTS). To define prestimulus effects of attention, we calculated mean firing in a 400-ms time window before stimulus onset, including

Fig. 1. General effects of attention. *A*: temporal sequence of events in the behavioral task. FP, fixation point; RF, classical receptive field. The pentagon and the triangle represent the cue stimuli instructing attention outside or inside the RF, respectively; bars represent the stimuli to be discriminated. *B*: each panel represents the behavioral performance of 1 monkey. Average accuracy (percentage of correct responses) and reaction times (RTs) as a function of %contrast are represented along the left and the right axes, respectively. Solid and dashed lines depict accuracy and RTs, respectively, for the orientation discrimination task performed inside (red) or outside (blue) the RF of the neuron under study; *n*, no. of averaged sessions. Only 1 data point is shown for *monkey F* in the attention-outside condition because the contrast was set to be constant (20%; see MATERIALS AND METHODS). *C*: average RTs measured for the orientation task performed outside the RF as a function of the distracter contrast (i.e., the contrast of the stimulus inside the RF, as shown on the *x*-axis). For *monkey F*, performance is shown for the task executed on the intermediate contrast (20%; solid blue line; see MATERIALS AND METHODS). For *monkey T*, instead, performance is shown for the task executed on a low contrast (5%; dotted blue line) or a high contrast (80%; dashed blue line). *D*: PSTHs are plotted for 4 representative levels of contrast and aligned with stimulus onset for a monotonically saturating (*top* panels) and a contrast-selective (*bottom* panels) single-cell example. Blue and red lines represent neuronal responses in the unattended and attended conditions, respectively. *E*: population PSTHs are shown for 6 logarithmically spaced levels of contrast for the whole population of cells; conventions are as in *D*. *P < 0.05; **P < 0.01, significant differences in firing between the attended and unattended conditions in 100-ms consecutive windows (Wilcoxon Mann-Whitney test). *F*: population averaged latency (in ms) is plotted as a function of %contrast when attention was allocated outside (blue) or inside (red) the RF. Each point represents the average (mean ± SE) across neurons.

all trials recorded in the unattended and in the attended condition separately.

To directly compare effects of attention on responses to different contrasts, we plotted responses to attended stimuli against responses to the same stimuli when they were unattended. To model the relationship between data points, we used a linear regression analysis, employing ordinary least squares as the estimation method. The analysis of regression slope (employing the firing in the unattended condition as the independent variable and the firing in the attended condition as the dependent variable) allowed us to establish which attentional mechanism was in place within a given time period, because different gain functions are expected to distribute responses in different ways (see RESULTS). Firing, as calculated in each window of interest (90-ms consecutive windows or 20-ms sliding windows for fine-grain temporal analyses; see above), was normalized to the population strongest response across contrasts and conditions in that epoch (note that results were fully consistent between the normalized and the nonnormalized version of this analysis). Linear correlation was significant for all tested windows ($P \ll 0.01$). To assess consistency of the results across cells in the population, we applied a subsampling method (Politis and Romano 1994). Specifically, random subsamples of cells were extracted (without replacement) 10,000 times from the original population, with the size of the subsample corresponding to around two-thirds of the size of the population of interest (200 cells in each sample for analyses on the whole population, 150 cells in each sample for analyses on neurons with homogenous contrast sensitivity, and 100 cells in each sample for analyses on subpopulations of neurons, respectively with or without baseline shift; see RESULTS), and the slope was computed as a function of time for each subsample. Confidence intervals were computed as means $\pm z(\alpha) \cdot$SD (DiCiccio and Efron 1996) from the 10,000 newly generated subsets. To estimate the significance of the temporal trends in the gain modulation for the whole population of cells, Gaussian random vectors were generated by using the means and variances estimated from the subsampling procedure (Sripati and Johnson 2006). As a result, these random vectors have no temporal trends. We then performed a multivariate analysis of variance between the bootstrap data and the randomly generated data to determine the significance of the observed trends in the temporal unfolding of model slope values (Sripati and Johnson 2006).

Single-neuron CRFs were determined for each cell using a non-weighted, least-squares fitting procedure (MATLAB, curve fitting tool "cftool"). The mean firing rate of each neuron was fitted to an extension of the traditional Naka-Rushton function (Albrecht and Hamilton 1982), namely, the Peirce function (Peirce 2007):

$$Response = R_{\max} \frac{C^n}{\left(C_{50}^{sn} + C^{sn}\right)} + base,$$

where $R_{\max}$ is the firing rate at which the curve asymptotes (note that it corresponds to the maximal response for monotonic functions), "base" is the undriven activity, C_{50} is the semisaturation contrast (i.e., the contrast value needed to reach half of the maximal response rate), the exponent n represents the slope of the curve, and s is the suppressive exponent. When s assumes a value of 1, the function corresponds to the traditional Naka-Rushton function, whereas higher values of s indicate nonmonotonic patterns. We used s to label cells as traditional monotonic or contrast selective; to be conservative, we considered a cell to be selective when $s > 1.1$ (Sani et al. 2013). We evaluated the goodness of fit by calculating the R^2 value (1 − SSE/SST, where SSE is the sum of squares error and SST is the sum of squares totals). Results were described and further analyzed only for well-fitted cells in both attentional conditions ($R^2 > 0.7$). In all analyzed temporal windows, both the unattended and the attended responses of individual cells were fitted almost equally well by the Peirce function (median explained variance, respectively, 92% and 91% in the early window, 80% and 82% in the intermediate window,

and 75% and 77% in the late window; a decrease in explained variance over time is likely due to the global decay of neuronal responses). Attentional effects on single-neuron CRFs were quantified by calculating the attention index (AI) for each relevant parameter as follows:

$$\frac{\left(Parameter_{attended} - Parameter_{unattended}\right)}{\left(Parameter_{attended} + Parameter_{unattended}\right)}.$$

In addition to base, we evaluated $R_{\max}$, C_{50}, and slope for traditional cells, whereas peak height, shift, and width were derived from the equation for contrast-selective cells. Specifically, we calculated shift (or peak contrast) as the contrast at which the maximal response occurred, and width (or bandwidth) as the difference between the two contrast levels at which the response was three-fourths of the maximal response, corresponding to 25% inhibition; note that a minority of nonmonotonic cells showed an inhibition lower than 25%, and their bandwidth could not be measured.

For a subset of cells, we additionally quantified the degree of monotonicity through the monotonicity index (MI; Ledgeway et al. 2005):

$$1 - \frac{\left(R_{\max} - R_{100}\right)}{\left(R_{\max} - R_0\right)},$$

where $R_{\max}$ is the maximum response of the neuron, R_{100} is the response to the maximal contrast used, and R_0 is the response to the null stimulus. MI assumes the value of 1 when the response is monotonically increasing (i.e., the response to the highest contrast is the maximal response of the neuron); it is smaller than 1 when the pattern is nonmonotonic (i.e., the response to the highest contrast is not the maximal response of the neuron).

Population CRFs were determined by averaging firing across selected cells and fitting the Peirce equation to the resulting data. To properly evaluate population effects for contrast-selective cells, we aligned the CRFs of all units to their respective peak position in the unattended condition. We placed the data points along a normalized abscissa using the equation

$$\frac{peak\ position - contrast}{peak\ position + contrast}$$

and averaged firing within 0.2 bin width. By aligning peak values of all units to the zero point (see RESULTS), as is conventional in the construction of population tuning curves for other visual features, this procedure enables the assessment of attentional effects at the peak and along its flanks for the whole population.

RESULTS

We trained two adult macaque monkeys to discriminate the orientation of achromatic bar stimuli in return for juice reward (Fig. 1A; see MATERIALS AND METHODS). In separate alternating blocks, the animals were instructed to covertly direct attention to either of two bars simultaneously presented on the screen, one inside and one outside the RF of the recorded neuron, while keeping central fixation. The bar inside the RF was displayed at various contrasts selected randomly on each trial. The monkeys reached a high level of performance at the task, with accuracy exceeding 75% (except for responses to stimuli presented at 2.5% contrast) and short RTs, indicating that the animals responded confidently to the orientation at the cued spatial position while disregarding the other stimulus (Fig. 1B).

Because a principal aim of our study was to characterize the evolution of attentional effects over time, we performed a control analysis directed at verifying whether the relative

saliency of the distracter stimulus might produce rapid consequences on the dynamics of attentional allocation, in turn affecting behavioral performance. In particular, one might expect longer RTs when the animal is engaged in processing a low-contrast target at the attended location while a high-contrast distracter is presented at the unattended location (triggering strong bottom-up attentional capture; for review, see for example Theeuwes et al. 2010), compared with when the distracter has relatively low contrast with respect to the to-be-attended stimulus. Although several features of the paradigm were meant to ensure stable allocation of attentional resources in space (see MATERIALS AND METHODS), and extensive training rendered the animals highly proficient at the task (implying strong resistance to bottom-up attentional capture), we set out to directly control for this potential problem by using the following approach. RTs of correct responses were evaluated when the monkeys performed the task outside the RF as a function of distracter contrast, i.e., the contrast level of the stimulus inside the RF. Specifically, for *monkey F*, RTs for correct responses to the single, intermediate contrast level (20%) used for the task performed outside the RF (see MATERIALS AND METHODS) were assessed as a function of the variable distracter contrast inside the RF. As confirmed statistically ($P = 0.79$, Kruskal-Wallis test), we obtained a completely flat pattern of RTs across distracter contrasts (Fig. 1*C*). A similar approach was applied for *monkey T*, for which we could isolate more critical control conditions. In the latter case, in fact, RTs as a function of the (inside RF) distracter contrast were separately measured when the animal was performing the (outside RF) task on a relatively low (5%)- or high-contrast (80%) target stimulus. In both cases, we found no significant modulation of RTs as a function of distracter contrast ($P = 0.64$ and $P = 1$, respectively, for the 5% and 80% target contrast conditions, Kruskal-Wallis test; Fig. 1*C*). On the basis of the collected evidence, we could safely exclude any marked influence of relative saliency of the distracter on the dynamics of attentional allocation in our task.

We recorded responses of V4 neurons to different luminance contrasts while the animals were attending inside or outside the neuron's RF; 307 cells (172 from *monkey F* and 135 from *monkey T*) were selected for in-depth analysis on the basis of the quality and stability of recordings, and after verifying for the correct allocation of spatial attention (see MATERIALS AND METHODS). In what follows, we mainly report on responses elicited by an optimally oriented stimulus. A systematic characterization of CRFs in V4 using part of the data from the same experiment, but regardless of any effect of attention, has been published previously (Sani et al. 2013).

General effects of attention. Within the population of recorded neurons, single V4 units displayed heterogeneous attentional effects, varying in overall strength and impact on different contrast levels, while sharing similar temporal dynamics. Figure 1*D* shows the peristimulus time histograms (PSTHs) of two representative neurons, i.e., a traditional monotonic (Fig. 1*D*, *top*) and a contrast-selective cell (Fig. 1*D*, *bottom*; Sani et al. 2013). In the single-cell example shown in Fig. 1*D*, *top*, attention exerts a comparable enhancement for all contrast levels, whereas for the single-cell example shown in Fig. 1*D*, *bottom*, a selective boost of responses at low contrasts is evident. Interestingly, for the latter neuron, although firing is comparable in response to 2.5% and 80% contrast stimuli in

the unattended condition, the attentional effect is remarkably different for the same two contrast levels. Critically, for both neurons in Fig. 1*D*, the attentional modulation is weak in the rising phase of the visually driven response but grows stronger in later phases; interestingly, a baseline shift is also present before stimulus onset, especially for the neuron depicted in Fig. 1*D*, *bottom*.

To obtain a global assessment of attentional influences on neuronal firing, we averaged responses in the attended vs. unattended condition across the entire population of 307 recorded neurons (Fig. 1*E*). We detected different time epochs of potential interest: a significant positive modulation before stimulus onset, a weak or negative modulation at the visually driven response peak (especially for middle and high contrasts), and a strong positive effect at later phases of stimulus processing (~150 ms after stimulus onset). The late positive modulation remains strong for low contrasts up to ~350 ms poststimulus, whereas it tends to vanish for high ones. This pattern of results was fully confirmed after selecting neurons showing a statistically significant attentional modulation in the poststimulus phase ($n = 170$; as assessed by the Friedman test in a 0- to 300-ms time window poststimulus onset, $P < 0.05$), with the size of the effects being increased, as expected.

We then explored whether the latency of visual responses differed between the two attentional states (Fig. 1*F*; see MATERIALS AND METHODS). In line with the literature (Albrecht 1995; Gawne et al. 1996; Lee et al. 2007), we observed a significant reduction in response latency with contrast in both attention conditions ($P = 0$, Kruskal-Wallis test). We also found a slight but reliable latency reduction when attention was directed inside the RF (on average across contrasts: -1.53 ± 0.48 ms mean $\pm$ SE; $P = 0.002$, Friedman test), in agreement with a recent study reporting small (1–2 ms) but significant reductions in the latency of spiking and LFP responses in area V4 with attention (Sundberg et al. 2012; but see Lee et al. 2007).

Different attention gain mechanisms are engaged over time. On the basis of suggestive evidence for a critical time dependency of attentional effects at both the single-cell and the population level (Fig. 1, *D* and *E*), we systematically characterized the temporal dynamics of the attentional modulation. For each contrast we calculated normalized mean firing rate time-locked to stimulus onset in 20-ms windows shifted by 1 ms (see MATERIALS AND METHODS) and plotted firing as a function of time, separately for the unattended and the attended condition (Fig. 2*A*). The comparison between these two conditions confirmed that attention affects responses differently over time. To better distinguish these dynamic changes, we computed the difference in firing in the unattended vs. attended condition within each 20-ms window (Fig. 2*B*) and checked its statistical significance by applying nonparametric random permutation tests (Fig. 2*C*; see MATERIALS AND METHODS). Across the population, the difference is reliably positive before stimulus onset and for the zero-contrast stimulus condition, in line with previous findings (Buffalo et al. 2010; McAdams and Maunsell 1999; Luck et al. 1997; Reynolds et al. 1999). Interestingly, attention has a negative (or null) effect in early phases of visually driven activity and a strong positive effect in later epochs. The early drop in the attentional modulation (bluish area in Fig. 2*B*) is progressively weaker and delayed as

contrast decreases. Note that, for each contrast, there is a temporal coincidence between the visual response peak and the deepest drop in attentional modulation, suggesting that, at a specific point in time, top-down attentional signals and bottom-up visual drive are concurrently modulating V4 and that the bottom-up drive dominates neuronal firing. This finding is in agreement with the idea of a brief disruption of spatial attention induced by the onset of visual stimulation, as previously proposed (Hayden and Gallant 2005). Fully coherent

results were obtained when we analyzed data from the subpopulation of cells significantly modulated by attention (Fig. 2, *D–F*), as well as responses to the suboptimal orientation and data from the two monkeys separately (data not shown). To rule out a decisive contribution of latency differences to the described temporal dynamics of attentional modulation, we applied the same approach for the visual latency-corrected condition (see MATERIALS AND METHODS) and confirmed a negative difference in firing soon after response onset and a strong
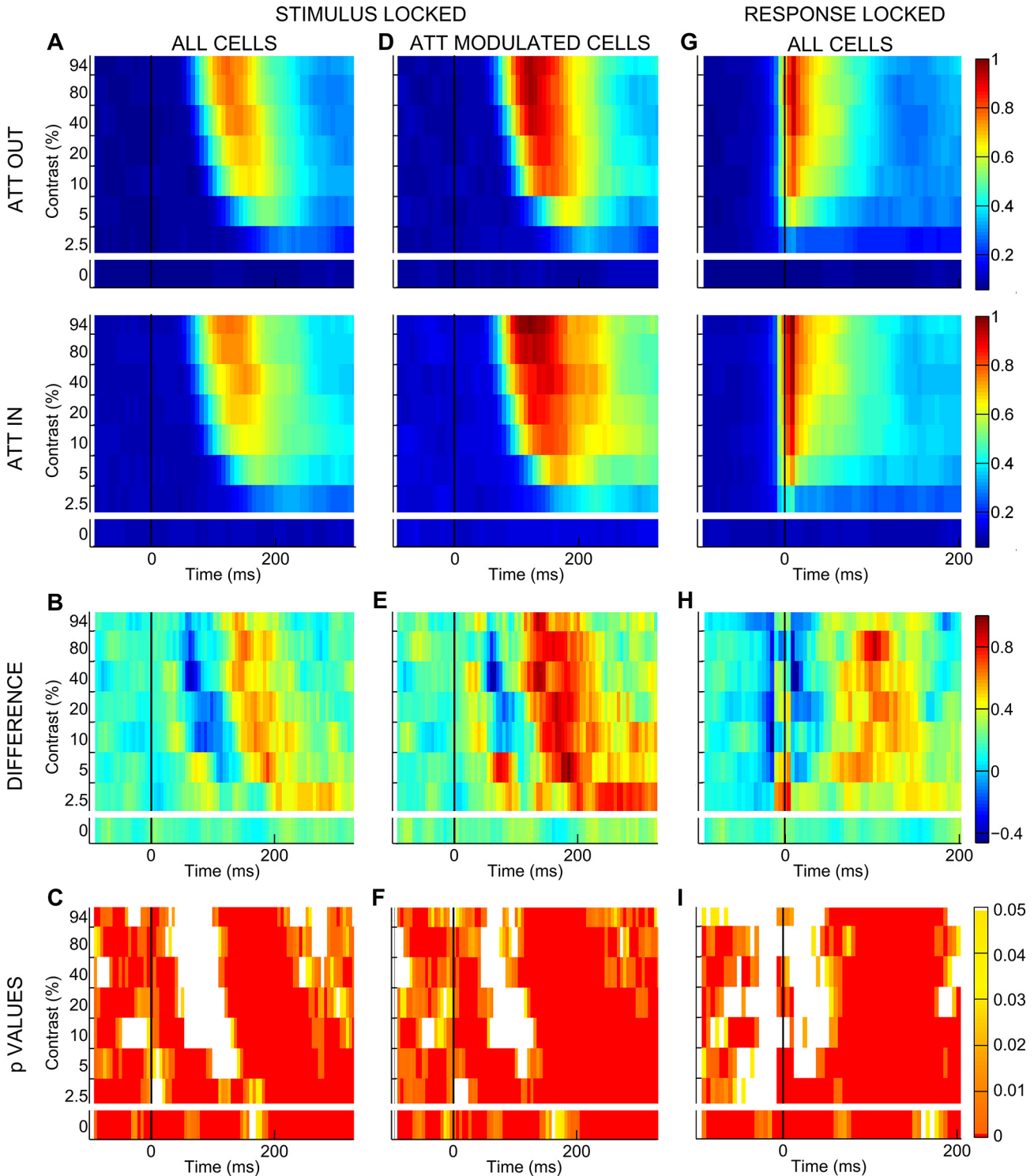
positive modulation in later epochs (Fig. 2, *G–I*). All subsequent analyses were performed on both stimulus-locked and latency-corrected data with a fully coherent pattern of results; in what follows, we mainly report results from the stimulus-locked conditions, unless otherwise stated.

We then tested directly the extent to which previously established attentional models (i.e., contrast gain, multiplicative, and additive models) could succeed in characterizing population effects, especially within distinct epochs of processing. We plotted population mean firing in the attended condition against mean firing in the unattended condition and analyzed the pattern of the data (Williford and Maunsell 2006). The diagrams in Fig. 3*A* show the theoretical patterns of response modulation according to the various models. Contrast gain would predict the greatest effect (maximum distance from the diagonal) for low and intermediate contrasts (slope <1; Fig. 3*A*, *left*), given the typical saturation of the CRFs at high contrast. Multiplicative gain would cause all responses to lie on a straight line that moves farther away from the diagonal as response strength increases (slope >1; Fig. 3*A*, *middle*). The additive model would predict all responses to lie on a straight line parallel to the diagonal (slope = 1; Fig. 3*A*, *right*). The slope of the regression of the attended against the unattended responses can be taken as a good index of the validity of the various models. We plotted the normalized population firing in the attended against the unattended condition for each 20-ms window and performed linear regression analyses (see MATERIALS AND METHODS). Figure 3*B* reports three example regression panels along with their respective CRFs. Each example confirms a clear correspondence between the slope value obtained in each epoch and the attentional effects over the CRF in the same epoch (see Supplemental Movie S1; supplemental material for this article is available online at the Journal website). To establish the prevalent gain mechanism in the population, we measured the regression slope as a function of time. As illustrated in Fig. 3*C*, a single gain model fails to describe the interaction between contrast and attention over time. Whereas in an early phase, the attentional effect appears to reflect a contrast gain mechanism (slope <1), the slope then increases well above unity, reaching a maximum around 150 ms after stimulus onset, consistent with a multiplicative gain model; in a later phase (~250 ms), the population slope again decreases below unity, consistent with the resurgence of a contrast gain mechanism.

To check whether the described dynamics of attentional effects (Fig. 3*C*) might (at least partly) originate from the time-varying influence of attention on different neurons within the population, e.g., depending on their basic visual properties, and in particular their contrast sensitivity (Williford and Maunsell 2006), we selected a subset of cells for which the value of C_{50} fell within a narrow range. Specifically, by applying fitting procedures to individual neurons (see MATERIALS AND METHODS), we observed that neurons in our data set were mostly characterized by high contrast sensitivity, corresponding to low values of C_{50} (Fig. 4*A*; see also Sani et al. 2013), as measured in the visually driven time window (30–120 ms after stimulus onset; see below). We then removed 21% of the cells (61 of 288 well-fitted cells) in the data set for which the value of C_{50} was higher than 15% contrast (Fig. 4*A*, open bars) and repeated the linear regression analyses as described above. As evident from Fig. 4*B*, the evolving intervention of attentional gain mechanisms over time was fully confirmed for neurons with more homogenous contrast sensitivity. Thus the alternation of different attentional gain mechanisms is not to be ascribed to the varying prevalence of effects on groups of cells with heterogeneous contrast sensitivity in different phases along the epoch of interest.

To further characterize how attention modulates responses of the whole population of neurons in our data set within three subsequent time epochs, each corresponding to the prevalence of a specific gain mechanism (Fig. 3*C*, gray shaded areas), we analyzed mean firing in an early (30–120 ms), an intermediate (120–210 ms), and a late window (210–300 ms) using stimulus-locked spike trains (Fig. 5*A*). As shown in Fig. 5*B*, where differences in firing between attentional conditions are plotted as a function of contrast, each temporal window reveals a distinct pattern of modulation, consistent with the notion that different attentional mechanisms intervene over time. Specifically, attention mainly enhances responses at low contrasts in the early epoch (Fig. 5*B*, *left*), in line with a contrast gain model (no significant modulation is found at the highest contrast; $P = 0.59$, Wilcoxon-Mann Whitney test); however, the enhancement observed for the lower contrast differs only marginally from that observed for the null stimulus ($P = 0.09$). In the intermediate time window, attention boosts responses at all contrast levels (Fig. 5*B*, *middle*); critically, the enhancement is greatest for 10% contrast, which yields the maximal response in the unattended condition (Fig. 5*C*, dark gray curve; note that the maximal population response in this case is not obtained for the highest contrast level, due to the presence of a substantial proportion of cells in the sample showing selective tuning for contrast; Sani et al. 2013; see below), and this effect is significantly larger than that observed at 2.5% contrast ($P = 0.01$), as predicted by a multiplicative

Fig. 2. Temporal dynamics of attentional modulation. *A*: for each contrast level, normalized population firing (surface color coding) in the stimulus-locked condition is shown as a function of time for the entire population of recorded cells. *Top* panel shows responses recorded in the unattended condition (ATT OUT), whereas *bottom* panel reports responses recorded in the attended condition (ATT IN). Responses were calculated in 20-ms windows, shifted by 1 ms. Note that average population firing rates were normalized to the maximum population firing across all contrasts and conditions shown. *B*: normalized firing difference between the attended and unattended condition over time is reported separately for each contrast level; color bar at *far right* represents the correspondence between firing difference values and surface color coding for *B*, *E*, and *H*. *C*: reliability in time of the observed attentional modulations is indicated by the *P* value associated with the given modulation, as assessed by nonparametric random permutation tests (see MATERIALS AND METHODS). Color bar at *far right* represents surface color coding of the represented *P* values for *C*, *F*, and *I*: white color surfaces correspond to nonsignificant spike differences between the attended and unattended conditions, whereas dark red surfaces correspond to $P < 0.0008$. *D–F*: cells significantly modulated by attention. Stimulus-locked, normalized population firing in the attended and unattended conditions (*D*), normalized firing difference between the 2 conditions (*E*), and reliability of the observed attentional modulations (*F*) are reported for the subpopulation of cells showing a significant attentional modulation (see text). *G–I*: visual response-locked (latency corrected) analyses. Normalized population firing in the attended and unattended conditions (*G*), normalized firing difference between the 2 conditions (*H*), and reliability of the observed attentional modulations (*I*) are reported for the entire population of recorded cells, after correction for differences in response latency, i.e., time-locked to visual response onset (see MATERIALS AND METHODS).
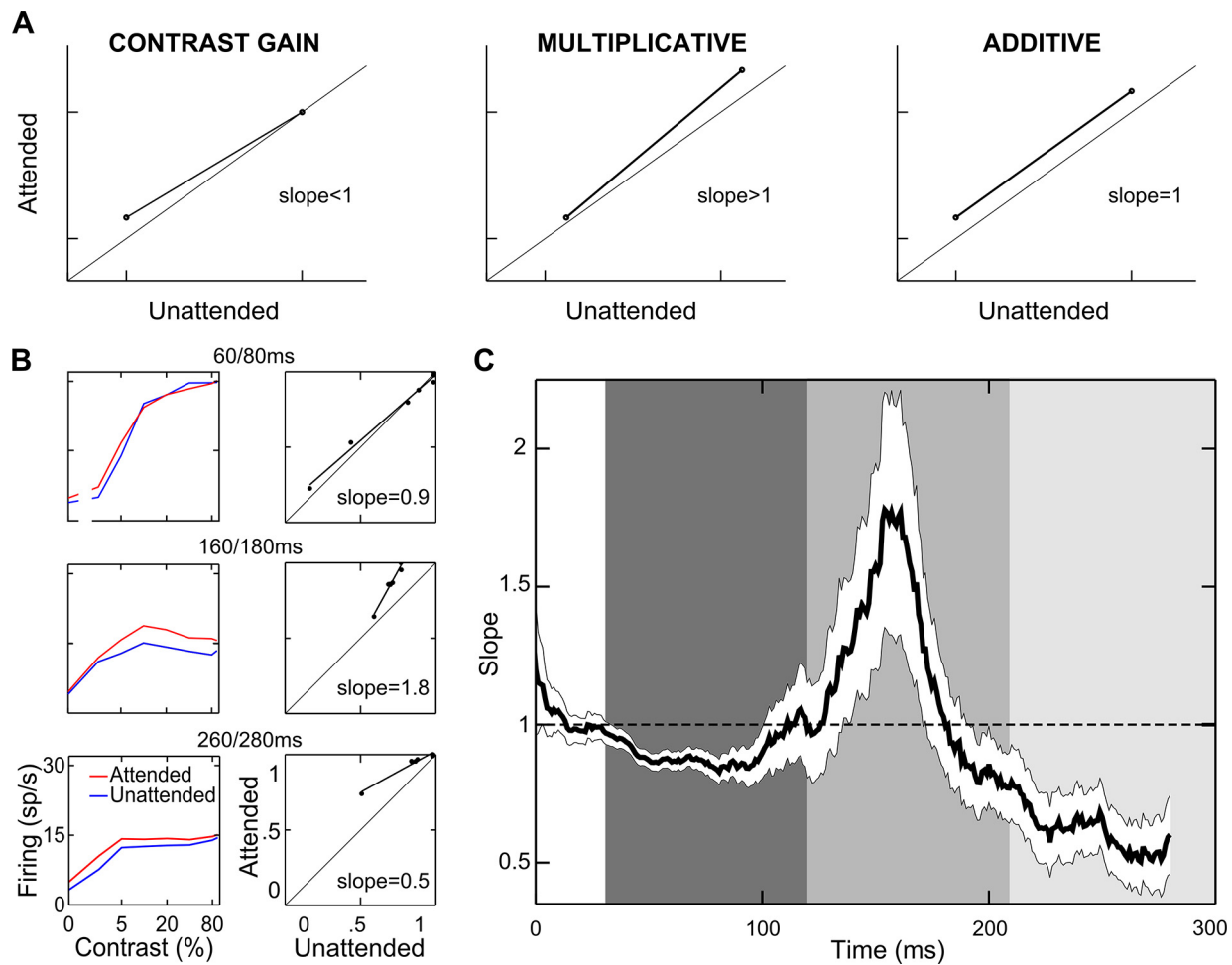
Fig. 3. Attentional models. *A*: schematics of how responses should be distributed if attention caused a pure contrast gain, multiplicative gain, or additive effect (see text). *B*: population normalized firing rates for each contrast in the attended vs. unattended condition are plotted for three 20-ms windows, time-locked to stimulus onset (*right* panels). Each point represents the average population response to a single contrast level, lines represent the linear regression for the plotted points ($P < <0.01$), and labels report the regression slope, whose value is diagnostic to decide which attentional model best describes data within each window. *Left* panels represent corresponding population CRFs in the attended (red) and unattended (blue) conditions. *C*: time course of the attentional effects. Slope values of the regression lines calculated within each 20-ms window are plotted as a function of time; the white ribbon indicates 95% confidence intervals computed using a subsampling procedure (with the size of each subsample corresponding to 200 cells; see MATERIALS AND METHODS). Shaded vertical rectangles highlight 3 consecutive temporal windows of particular interest (see text). Note that temporal trends were significant (multivariate ANOVA, $P < 0.0005$; see MATERIALS AND METHODS).

rescaling of the CRF. In the late epoch (Fig. 5*B*, *right*), again attention predominantly strengthens responses to middle and low contrasts; in this case, the modulation for 2.5% contrast is significant ($P < 0.0001$), and, differently from what is obtained in the early epoch, it is also reliably larger than that observed for the null stimulus ($P = 0.02$). A compatible pattern of attentional modulation as a function of contrast and time window is reported for the latency-corrected data (Fig. 5, *D* and *E*). Note that the divergent pattern of modulation within the intermediate and late epochs can hardly be the direct consequence of differences in firing across the two time epochs, because the CRFs obtained in the unattended condition (Fig. 5, *C* and *F*) are highly similar across these two epochs (especially in the latency-corrected condition).

Interestingly, not only are the attentional effects profoundly different in nature over subsequent phases of visual processing at the population level, but also the number of single cells contributing significantly to the attentional effects changes over time and is maximal in the multiplicative phase. We

statistically assessed poststimulus attentional modulation in the three epochs of interest by applying a Friedman test ($\alpha = 0.05$) with contrast and attention as main factors. In the early time window, 47 cells (22.5%) were modulated by attention; the number was more than doubled in the intermediate window (136 cells; 44.3%) and still substantial in the late window (105 cells; 34.2%).

Attention and heterogeneous contrast coding: evidence from single-cell analyses. Contrast coding across neurons in area V4 shows considerable variability along a continuum (Sani et al. 2013). We assessed whether the pattern of attentional modulation we described for the entire population reliably held for neurons that encode contrast in a distinct manner (i.e., for cells with traditional monotonic CRFs and for contrast-selective cells). For each of the three time windows of interest, single-neuron CRFs were fitted by the Peirce equation, which is able to accommodate for both kinds of contrast coding by virtue of a suppressive exponent (Peirce 2007; see MATERIALS AND METHODS). The sample of recorded neurons
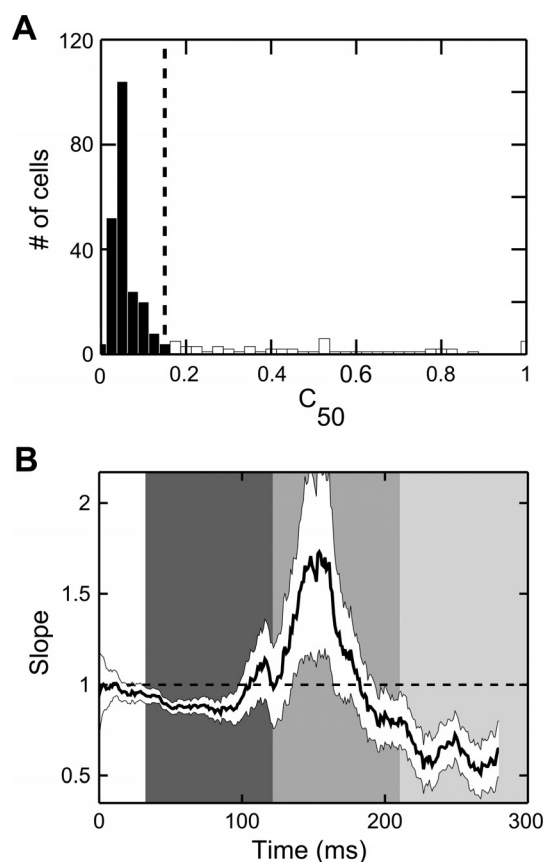
A

B

Fig. 4. Negligible impact of varying single-cell contrast sensitivity on the overall dynamics of attentional effects. *A*: histogram represents the distribution of C_{50} across the population of recorded neurons, as assessed during the visually driven temporal window (30–120 ms after stimulus onset) in the unattended condition. The dashed vertical line represents the cutoff value (15% contrast) used for the subsequent control analysis. Note that most of the cells in the population showed high contrast sensitivity (Sani et al. 2013), corresponding to low values of C_{50} (filled bars), whereas only a minority of cells (61 cells, 21% of the 288 well-fitted cells in the considered epoch/condition; open bars) showed low and variable contrast sensitivity. *B*: time course of the attentional effects measured for cells with relatively uniform contrast sensitivity. Slope values of the regression lines calculated within each 20-ms window are plotted as a function of time for the subpopulation of cells showing a value of C_{50} lower than 15% contrast; the white ribbon indicates 95% confidence intervals computed using a subsampling procedure (see MATERIALS AND METHODS). Conventions are as in Fig. 3*C*.

showed a certain degree of variability both in the overall strength and distribution of attentional effects across contrasts, as previously described in macaque V4 and other cortical visual areas (Martínez-Trujillo and Treue 2002; Reynolds et al. 1999; Thiele et al. 2009; Williford and Maunsell 2006). Specifically, Fig. 6*A*, 1st and 2nd panels, depicts two traditional single-cell examples modulated through a contrast gain or a multiplicative gain in the intermediate window, respectively. Importantly, and new to the field, we found contrast-tuned neurons to be strongly modulated by attention (Fig. 6*A*, 3rd and 4th panels); this modulation appeared to be mainly exerted through a multiplicative gain mechanism, but some neurons did show a contrast gain-like modulation, wherein the response peak was shifted toward lower contrast levels.

We therefore separately considered the subpopulations of cells showing traditional (monotonic) or selective (tuned) CRFs in both attentional conditions, as established on the basis

of the suppressive exponent of the fitted equation (Sani et al. 2013), and quantified attention-dependent variations of critical CRF parameters due to attention using an attention index (AI) calculated for each parameter (see MATERIALS AND METHODS). Consistent with the results at the whole population level, monotonic cells showed contrast gain modulation in the early window, with a significant decrease in C_{50}, or the semi-saturation contrast (Fig. 6*B*, *left*), and a leftward shift of the average population curve (Fig. 6*C*, *left*). On the contrary, R_{max} values (i.e., responses to highest contrasts) significantly increased in the intermediate window (Fig. 6*B*, *middle*), corresponding to an upward shift of the average population curve and reflecting a multiplicative gain modulation (Fig. 6*C*, *middle*). Finally, in the late window, we found a reduction of C_{50} and a significant increase of the slope (Fig. 6*B*, *right*); the attentional effect was stronger for low and intermediate contrasts (Fig. 6*C*, *right*), thus confirming a contrast gain modulation.

A compatible pattern of results was found for contrast selective neurons, although with some peculiarities. Specifically, the attentional modulation in the early window was rather weak and limited to a significant baseline enhancement (Fig. 6*D*, *left*). However, a nonsignificant leftward shift of the peak, which was on average slightly lower and narrower, could be described (Fig. 6*E*, *left*). Similarly, the attentional modulation of fitted parameters in the late window was generally consistent with the described enhancement of responses to middle and low contrasts of the overall population (although not reaching statistical significance for this subgroup of cells); in fact, variations of the equation parameters with attention show that the peak position slightly shifted to the left and peak width decreased (Fig. 6*D*, *right*). Consistently, the mean re-aligned population curve reveals an enhancement of the left flank of the tuning function (Fig. 6*E*, *right*). Finally, an attentional multiplicative modulation was evident in the middle window, with a significant increase in peak height (Fig. 6*D*, *middle*); the average population curve shows that attentional effects are spread across all contrast levels, being however slightly higher at the peak (Fig. 6*E*, *middle*). A further analysis revealed that what appears to be, on average, an additive effect in this window is actually due to the attentional modulation being typically stronger at the peak, and also sometimes stronger along one of the two flanks of the tuning curve. To address this point, for each selective neuron, the AI on firing rate was calculated separately for contrasts lower (AI low) and higher (AI high) than the preferred one, as established in the unattended condition (Fig. 7*A*); the scatter plot compares the attentional modulation exerted on the left (AI low) vs. right (AI high) flank of the tuning function. Note that most points are distributed along the diagonal, in line with the observation of a comparable attentional modulation along the two flanks of the tuning curves; in fact, a reliable correlation emerges in the strength and direction of the attentional modulation over the two flanks of the tuning curve ($P = 0.001$). However, there is a considerable degree of variability (see Fig. 7, *B–D*), with points far away from the diagonal and almost equally distributed on the two sides of it, meaning that at least a subset of contrast-selective cells show stronger enhancement for one flank than the other of the tuning curve. Such asymmetric effects at the single-cell level might well account for the quasi-additive effect observed at the population level (Fig. 6*E*, *middle*). Interestingly, the asymmetry of the attentional mod-
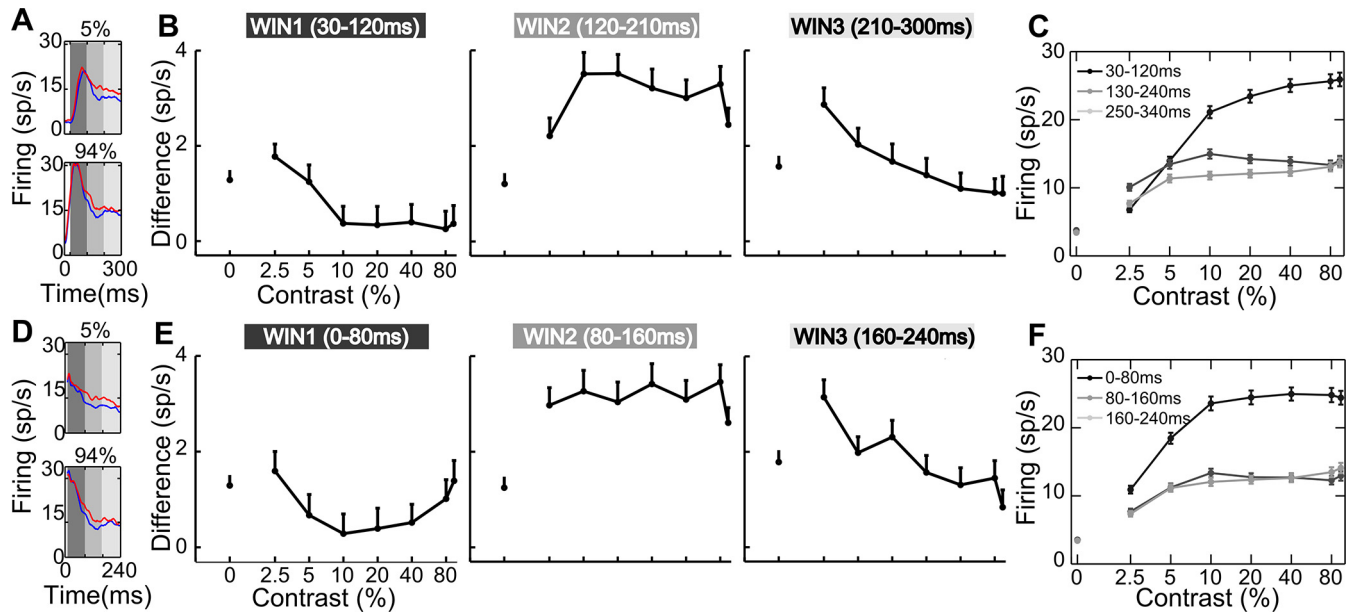
Fig. 5. Early, intermediate, and late epochs. *A* and *D*: population PSTHs time-locked to stimulus onset (*A*) and to visual response onset (*D*) are plotted for 5% and maximal contrast in both the attended (red) and unattended (blue) conditions. The gray shaded areas represent critical time windows: early (30–120 ms), intermediate (120–210 ms), and late (210–300 ms). *B* and *E*: average response difference (sp/s, spikes/s) is plotted as a function of contrast for the early (*left*), middle (*middle*), and late windows (*right*), using stimulus-locked (*B*) and visual response-locked (*E*) spike trains. Vertical lines represent SE. *C* and *F*: population CRFs in the unattended condition are shown for each temporal window aligned to stimulus onset (*C*) and visual response onset (*F*).

ulation is negatively correlated with peak position along the contrast axis ($P = 0.02$) such that cells with a preference for very low contrast values tend to show a stronger modulation of the right flank of the tuning curve (Fig. 7*C*), and vice versa, neurons with a preference for high contrast values tend to show a stronger modulation of the left flank of the tuning curve (Fig. 7*D*). In brief, for selective cells, we found only a modest modulation, mainly exerted on the left flank of the tuning function, in the early phase, whereas a clearer contrast gain modulation emerged during the late phase. Maximal effects of attention, however, were expressed during the intermediate epoch, where responses were multiplicatively rescaled, with the strongest modulation occurring at peak contrast; in some cases, a more pronounced effect was found along one of the two flanks of the curve, in turn related to the peak position for the given neuron. Interestingly, the described multiplicative modulation is similar to that exerted by attention over other basic visual features, such as orientation (McAdams and Maunsell 1999).

Consistent with previous work (e.g., Lee and Maunsell 2010; Williford and Maunsell 2006), results at the single-cell level showed a certain degree of variability. Nonetheless, the temporal unfolding of gain mechanisms described for the entire population, as well as for monotonic and selective cells, was further confirmed at the level of individual neurons, as can be appreciated by the following approach. We plotted single-cell changes induced by attention on the critical parameters distinguishing contrast gain and response gain accounts of attentional effects, separately for the early (Fig. 8*A*), intermediate (Fig. 8*B*), and late time epochs (Fig. 8*C*). The AI for C_{50} (monotonic cells; filled circles) or peak contrast (selective cells; open circles) is reported on the *x*-axis; (leftward) shifts in this parameter are the signature of a contrast gain effect of attention. The AI for R_{max} (monotonic cells; filled circles) or peak height (selective cells; open circles) is reported on the

y-axis; (upward) shifts in this parameter are the signature of a response gain effect of attention. Despite variability of the results across single cells in the population, we could confirm a prevalence of a contrast gain effect in the early (Fig. 8*A*) and late windows (Fig. 8*C*), as shown by a leftward shift in the C_{50}/peak position distribution (WIN1: AI = -0.06 ± 0.02, mean $\pm$ SE, $P < 0.001$, Wilcoxon signed rank test; WIN3: AI = -0.11 ± 0.05, $P < 0.05$; see histograms above the plots). In both the early and late epochs, instead, no clear bias could be detected for attention-induced variations in maximal firing, which was either reduced or increased with similar probability across the population (WIN1: AI = 0 ± 0.01, $P = 0.51$; WIN3: AI = 0.02 ± 0.03, $P = 0.63$; see histograms to the right of the plots). Conversely, in the intermediate time window (Fig. 8*B*), a prevalence of a response gain effect, i.e., of increases in R_{max}/peak height, was observed (the histogram to the right of the plot shows a clear bias toward positive AI values; WIN2: AI = 0.08 ± 0.03, $P < 0.01$). Leftward and rightward shifts in C_{50}/peak position were instead observed with equal probability across the population during this epoch (the distribution of this parameter was symmetrical around zero; WIN2: AI = -0.01 ± 0.05, $P = 0.66$; see histogram above the plot).

In conclusion, the temporal dynamics of attentional modulation, as described for the whole population (Figs. 3 and 5), was evident for both traditional and contrast-selective cells (Figs. 6–8), thus demonstrating that neurons with different coding properties are mainly modulated through two types of gain function that occur sequentially. At any rate, such homogeneous temporal dynamics of attentional effects among neurons with different patterns of contrast selectivity suggests a similar contribution of those different cell classes to the overall attentional effects and provides further insights regarding the mechanisms underlying contrast coding and attention, and their interaction (see DISCUSSION).
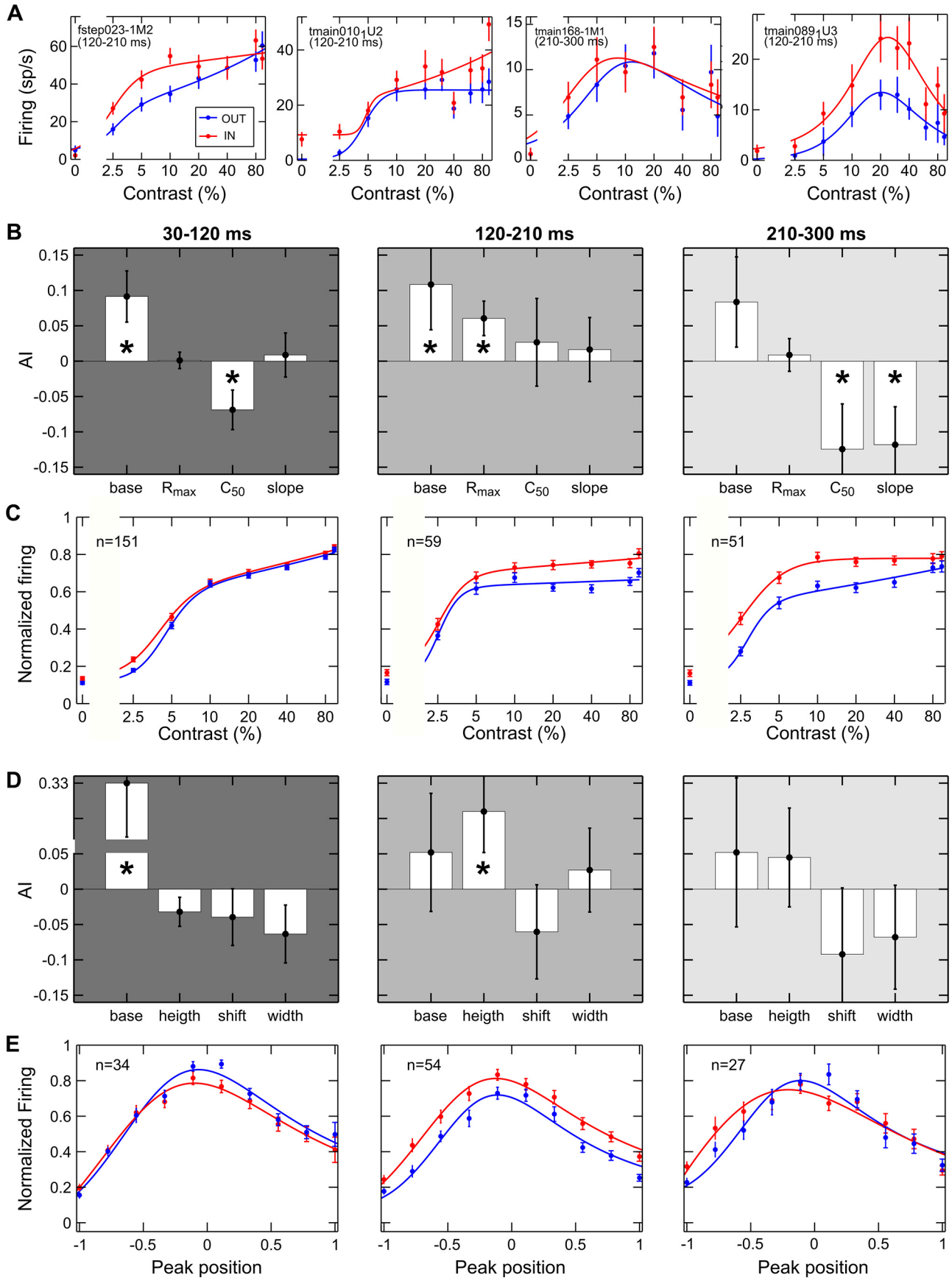
Fig. 7. Modulation of contrast-selective cells during the multiplicative stage. *A*: scatter plot comparing the single-cell attention index (AI) separately for responses to contrasts lower (AI low) and higher (AI high) than the preferred one, as established in the unattended condition. Histograms represent the distribution of AI for the contrast higher (*right* plot) and lower (*top* plot) than the preferred one. Red dots represent the position in the scatter plane of the 3 single-cell examples shown in *B–D*. *B–D*: attentional modulation of contrast-selective cells (same conventions as in Fig. 6*A*). Data in *B* represent an example neuron lying on the diagonal and thus showing symmetric attentional effects of attention on the 2 flanks of the tuning function, i.e., a pure multiplicative effect. Data in *C* represent an example neuron lying on the left of the diagonal (*top left* quadrant), thus showing a stronger effect of attention on the right flank of the tuning function (i.e., for contrasts higher than the peak). Data in *D* represent a contrast-selective neuron lying on the right of the diagonal (*top right* quadrant), thus showing a stronger attentional effect for contrasts lower than the peak. In all cases, the largest effect in this temporal window (intermediate epoch) mainly occurs for the contrast level eliciting the maximal response, thus confirming a multiplicative rescaling of neuronal responses. Interestingly, in the examples shown in *C* and *D*, the asymmetry in the attentional modulation along the flanks of the tuning curve appears to be related to peak position in the given neuron, as confirmed by quantitative analyses (see text).
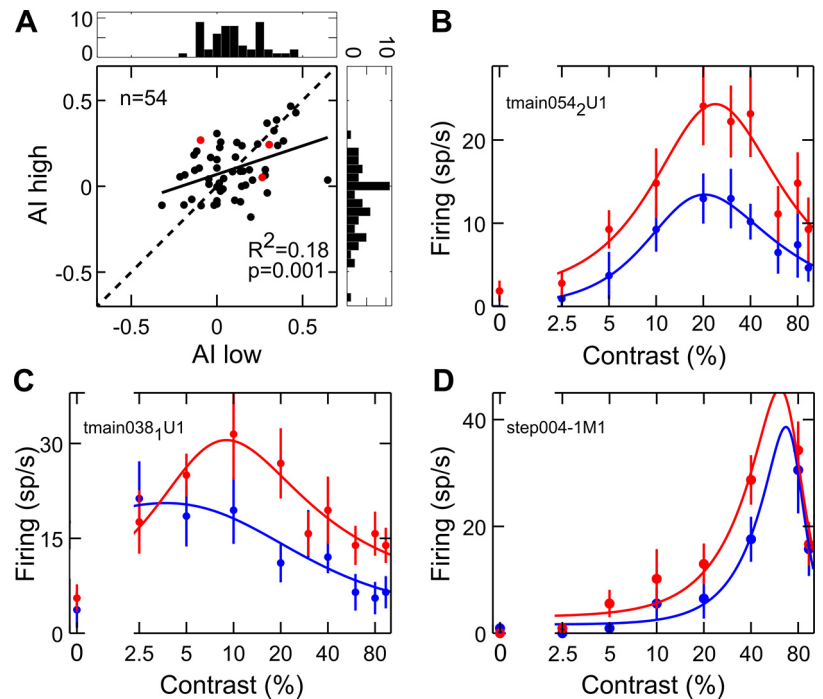

Unexpectedly, attention was also able to alter the overall pattern of responses to varying contrast (CRF shape) in a substantial number of cells (respectively, 32%, 36% and 36% of the total well-fitted cells in each of the critical time epochs): attention could either convert a traditional monotonic CRF into a contrast-tuned cell, i.e., a peak appeared (Fig. 9*A*, *left*; see also Fig. 5*C* from Williford and Maunsell 2006 for a compatible cell example), or convert contrast-selective, tuned responses into a traditional profile, i.e., the peak disappeared (Fig. 9*A*, *right*). This effect was evident as a strong change in the value of the suppressive exponent of the Peirce function that defines the shape of the CRF (Fig. 9*B*), as well as in the monotonicity index (Fig. 9*C*; see MATERIALS AND METHODS). In each of the three critical epochs, there were two consistent groups of neurons of roughly the same size, fitted comparably well and with a change in shape of comparable strength in either of the two directions, as assessed by these parameters. Although further investigations are required to better understand the observed phenomenon, such radical changes in CRF profile might reflect the ability of attention mechanisms to optimize selectivity in the population of recruited neurons. In other words, in tasks where fine contrast discrimination/categorization is required or, vice versa, in tasks where contrast is completely irrelevant, attention might be able to turn CRF shape of a fraction of neurons into tuned or monotonic, respectively, ultimately optimizing task performance. In our experiment, monkeys performed an orientation discrimination task, with stimulus contrast contributing significantly to the discriminability of target stimuli, although it was task irrelevant; consistently, we found an ambiguous situation in which attention changed CRF shape of a fraction of neurons bidirectionally.

Contribution of pure top-down signals. In our experiment, the monkeys were informed of the behaviorally relevant location in advance of stimulus presentation (see MATERIALS AND METHODS). This enabled us to establish the extent to which top-down signals exert relevant anticipatory effects on baseline activity, as found in prior electrophysiological studies in monkeys (Buffalo et al. 2010; Luck et al. 1997; McAdams and Maunsell 1999; Reynolds et al. 2000) as well as in several human functional magnetic resonance imaging (fMRI) studies (Kastner et al. 1999; Li et al. 2008; Ress et al. 2000; Sylvester et al. 2009). For each cell, we compared firing activity in the attended vs. the unattended condition, over a 400-ms time window before stimulus onset (Fig. 10*A*). Whereas 156/307 cells (50.8%; Fig. 10*B*, *bottom*) were significantly modulated (Wilcoxon-Mann Whitney test, $P < 0.05$), 151 (49.2%; Fig. 10*B*, *top*) were not. For modulated neurons, average firing rate was 4.3 spikes/s in the attended condition and 3.5 spikes/s in the unattended condition, corresponding to a 24.6% increase in

Fig. 6. Effects of attention on different cell classes. *A*: a contrast gain (1st panel) and a multiplicative modulation (2nd panel) are reported for 2 example cells showing traditional monotonic CRFs. A contrast gain (3rd panel) and a multiplicative modulation (4th panel) are reported for 2 example cells showing selective CRFs. Mean firing rate (spikes/s) is plotted as a function of %contrast for the attended (red) and unattended (blue) conditions. Each point represents the average of ≥12 stimulus presentations, along with its SE (vertical lines). Solid lines depict the best fitted curve provided by the Peirce equation. Labels report the cell name and the temporal window used to calculate firing. *B*: attentional modulation of the average best fitted parameters of traditional monotonic cells. AI was calculated for parameters provided by the Peirce function for each neuron in both attentional conditions and then averaged across cells for the early (*left*), intermediate (*middle*), and late window (*right*). Vertical lines represent SE. *P < 0.05 indicates the mean of the AI distribution was significantly different from zero (Wilcoxon test). *C*: average normalized responses of cells showing a traditional CRF in both the attended (red) and unattended (blue) conditions are reported as a function of contrast for each time window. Vertical lines represent SE. Solid lines represent the best fitted curve provided by the Peirce function. *D*: attentional modulation of the average best fitted parameters of contrast selective cells; same conventions as in B. *E*: average normalized responses of cells showing contrast-selective responses in both attentional conditions are plotted after the CRFs of all units were aligned to their respective peak position in the unattended condition (see MATERIALS AND METHODS); same conventions as in *C*.
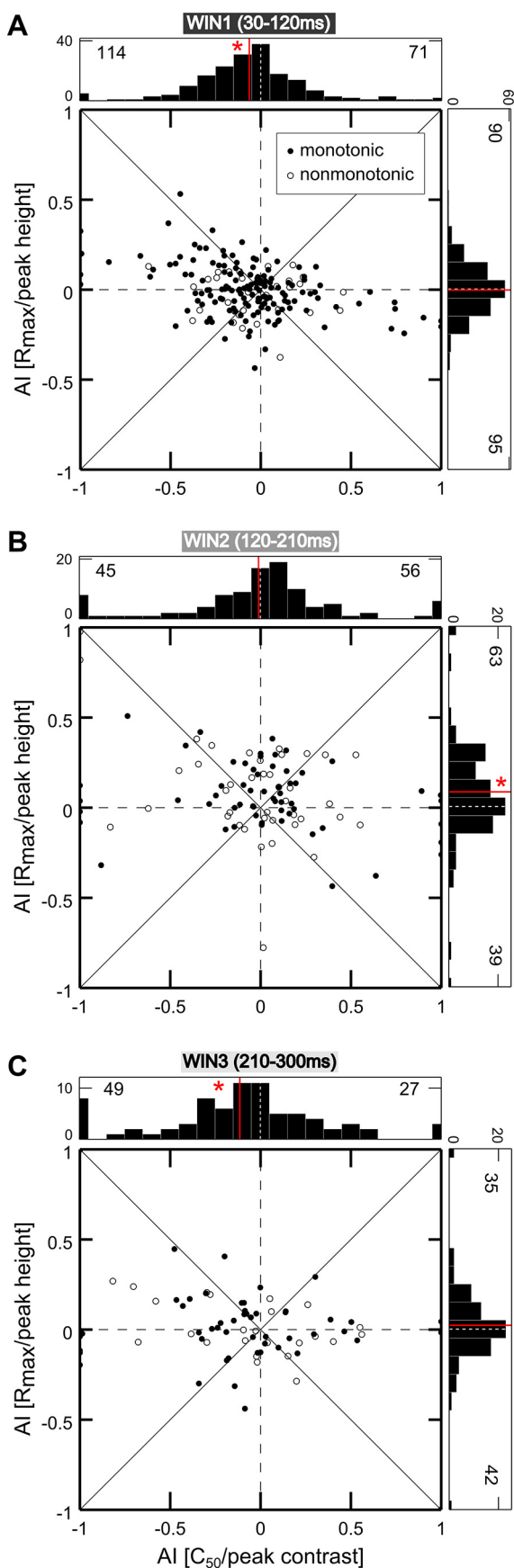
firing in the attended condition. The temporal evolution of the baseline modulation at the population level was analyzed by calculating firing in 100-ms time windows shifted by 25 ms (Fig. 10B, *middle*). Interestingly, attention to the RF progressively increases baseline activity, probably reflecting a growing effort in attentional deployment with time. Although this effect was strong in the subpopulation of cells showing a significant baseline shift (Fig. 10B, *bottom*), it was nearly absent in the subgroup of unmodulated cells (Fig. 10B, *top*).

We explored the contribution of purely top-down signals to the poststimulus effects of attention by analyzing the temporal dynamics of attention separately for the two cell populations, respectively with and without a reliable baseline shift. The progression of different gain mechanisms, as described for the general population (Fig. 3), was replicated in both subgroups, but with important differences. The multiplicative effect was stronger for cells without prestimulus modulation (Fig. 10C, black curve); in contrast, a magnification of the contrast gain modulation, in both the early and late windows, emerged for cells with a reliable baseline shift (yellow curve). To test for the reliability of these differences, we calculated the average, normalized firing in the attended vs. unattended condition in each of the 90-ms critical time epochs, separately for each subpopulation of cells, and applied a subsampling procedure to directly compare the slope values obtained with regression analyses (see MATERIALS AND METHODS); as a result, we confirmed a statistically significant difference between slope values obtained for the two subpopulations in each critical time window (Wilcoxon rank sum test; $\alpha = 0.05$).

Analysis of firing differences as a function of attention allowed for a deeper understanding of the effects in the two subpopulations (Fig. 10C, *insets a–f*). Cells without baseline shift (Fig. 10C, *insets a–c*) showed clear multiplicative rescaling of responses during the intermediate window (Fig. 10C, *inset b*), with maximal attentional enhancement for contrasts yielding higher responses in the unattended condition (Fig. 10D, *left*, dark gray curve). In line with the absence of prestimulus modulation for these cells, attentional modulation of activity in the poststimulus epoch was especially weak for the null stimulus, suggesting that multiplicative mechanisms depend heavily on effective visual drive (Ekstrom et al. 2008). The multiplicative rescaling of responses occurs in a delayed epoch relative to onset of visual responses, likely reflecting a recurrent stage of processing (see DISCUSSION). For this subpopulation of cells, in the early epoch, we observed a negligible spike difference for all contrasts tested (Fig. 10C, *inset a*),

Fig. 8. Attentional gain models and single-cell variability. *A–C*: scatter plots comparing single-cell AI for contrast sensitivity/contrast preference and AI for maximal response in the 3 critical time epochs, i.e., in the early (*A*), intermediate (*B*), and late window (*C*). Filled circles represent single cells showing a traditional CRF, for which AI for C_{50} and R_{max}, as obtained from the best fitting procedures, are compared. Open circles represent single cells showing a tuned CRF, for which AI for peak contrast and peak height, as obtained from the best fitting procedures, are compared. Histograms representing the distribution of AI for C_{50}/peak position across the population are shown above each plot, whereas histograms representing the distribution of R_{max}/peak height across the population are shown to the *right* of each plot. The red solid line in each histogram represents the average AI for the given parameter across the population (*$P < 0.05$, Wilcoxon signed rank test); numbers of cells with an AI value <0 (*left/bottom* parts of the histograms) and >0 (*right/top* parts of the histograms) are also reported on each graph.
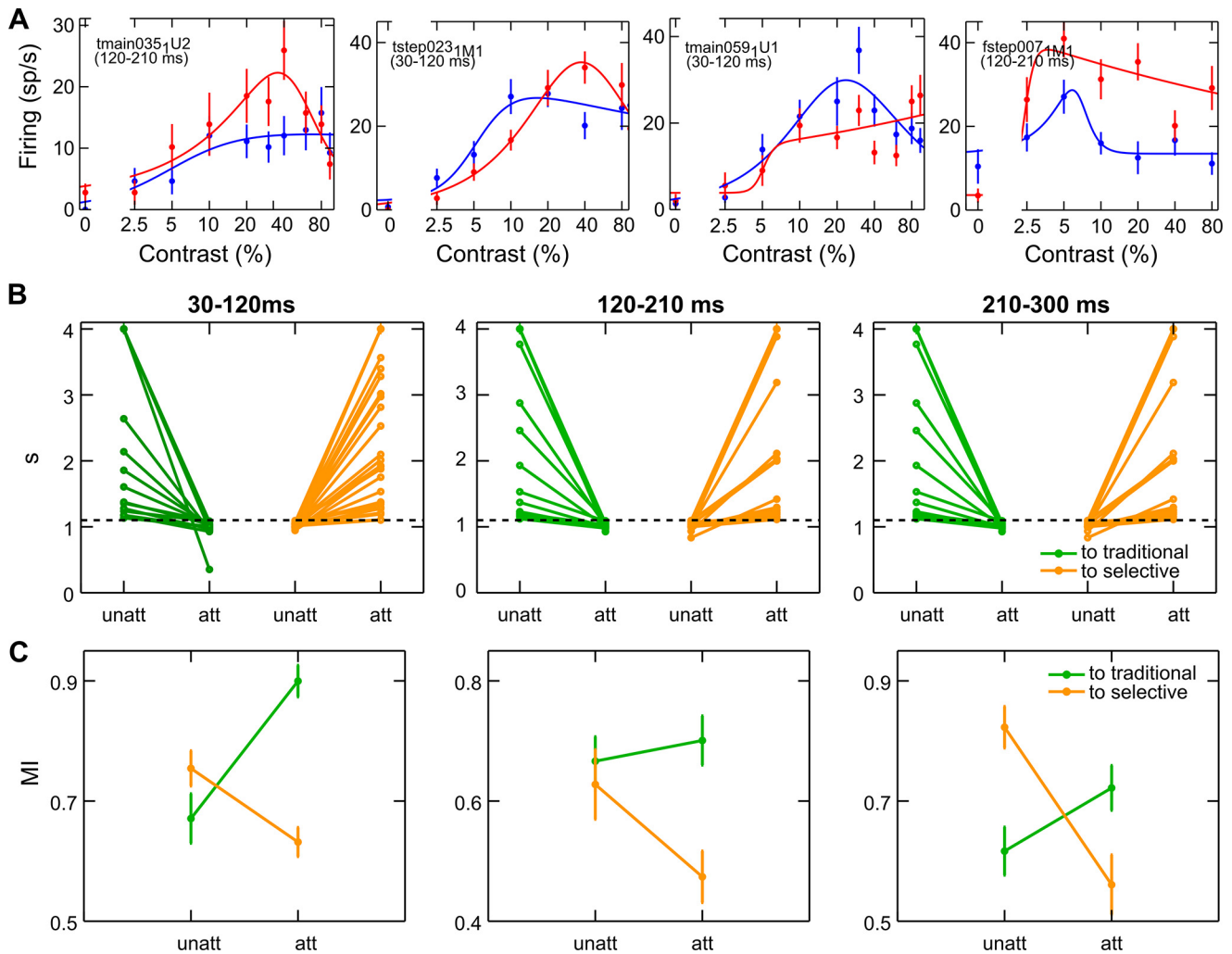
Fig. 9. Attention reshapes CRFs. *A*: the 2 *left* panels represent 2 example cells whose CRF shape turns from traditional to selective, whereas the 2 *right* panels represent 2 cells whose CRF shape turns from selective to traditional, as a consequence of attentional modulation; same conventions as in Fig. 6*A*. *B*: single-cell suppressive exponent is reported for the attended and unattended conditions, separately for cells turning to selective (green) and to monotonic (orange). *C*: single-cell monotonicity index (MI) is reported for the attended and unattended conditions; same conventions as in *B*.

whereas a tendency toward contrast-gain modulation could be detected in the late window, where attention exerted a maximal (although still marginal) effect for low-to-intermediate contrast levels (Fig. 10*C*, *inset c*).

In contrast, the subpopulation showing reliable baseline shift (Fig. 10*C*, *insets d–f*) was characterized by clear attentional effects for low contrast stimuli in all temporal windows. In the early epoch (Fig. 10*C*, *inset d*), the attentional modulation at low contrast levels was similar to that observed for the null stimulus, in line with the idea that a preexisting modulatory signal persists throughout the poststimulus phase for low contrast levels, where it appears to summate with the visual response. Compatible with a subadditive mechanism, the positive influence of the baseline shift becomes progressively weaker as the visual drive increases, eventually exerting no effect on neuronal responses in the saturating portion of the CRF. In the intermediate window, responses to high-contrast stimuli are boosted through a multiplicative gain mechanism; however, a strong attentional effect at low and intermediate contrast is still present in this phase, leading to an almost equal boost of responses to all contrasts (Fig. 10*C*, *inset e*). A resurgence of contrast gain can be observed in the late window,

but with a different pattern relative to that observed in the early phase; in this case, the late attentional enhancement of responses to low-contrast stimuli amply exceeds the effect measured for the 0% contrast stimulus (Fig. 10*C*, *inset f*). Notably, visual activity is still sustained in the late window across the whole contrast range (Fig. 10*D*, *right*, light gray curve), ruling out the possibility that lack of modulation in the high-contrast range might be ascribed to weak visual activity for higher contrasts in this window. The pattern of modulation in the late epoch is thus compatible with an effective contrast gain, corresponding to an appreciable increase in contrast sensitivity for this subpopulation of cells. An alternative, but not mutually exclusive, account of the late contrast gain modulation might be related to the different timing of the perceptual decision process along the contrast range, although we did not find direct evidence in favor of this hypothesis (see DISCUSSION).

Given the marked differences in the pattern of attentional modulation between the two subpopulations of neurons illustrated in Fig. 10*C*, we tried to gain a better understanding of the underlying mechanisms. First, we could exclude any impact of fundamental variations in contrast coding between the population of cells with and without a reliable baseline shift, because
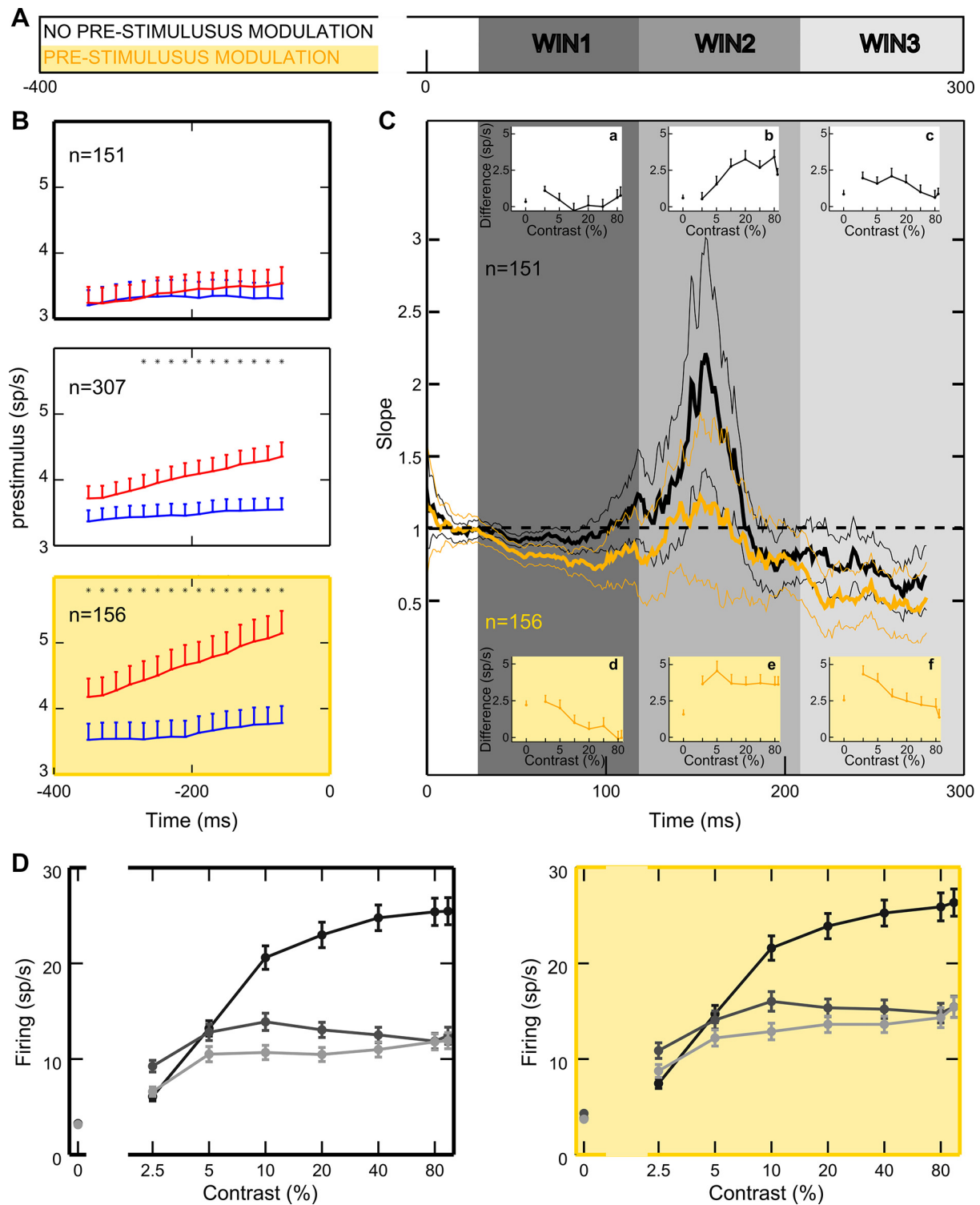
Fig. 10. Poststimulus modulation of attention interacts with prestimulus modulation. *A*: the bar illustrates the timeline and critical analysis windows: yellow and white bands show the time window used to analyze prestimulus modulation; gray bands show the early, intermediate, and late windows. *B*: time course of prestimulus modulation. Attentional modulation is calculated before stimulus onset in 100-ms windows, shifted by 25 ms, for the whole population (*middle*), for the population with (*bottom*) and without (*top*) a reliable baseline shift. *C*: time course of the attentional effects for the subpopulations of cells with (yellow) and without (black) a reliable baseline shift. Model slope values are shown as a function of time; thin lines delimit 95% confidence intervals computed using a subsampling procedure (with the size of each subsample corresponding to 100 cells; see MATERIALS AND METHODS). *Insets* show the spike difference between the attended and unattended condition in each window of interest, separately for the population of cells unmodulated (*insets a–c*, white background) and modulated by attention before stimulus onset (*insets d–f*, yellow background). *D*: unattended population CRFs for each temporal window locked to the stimulus onset are reported for the subpopulation of cells with (*right*) and without baseline shift (*left*).

this was highly similar across the two populations (Fig. 10D, *left* and *right*). Still, the two subpopulations of neurons might differ in other basic properties, such as neuronal type, cortical layer, and general excitability. Interestingly, in the unattended condition, we found a reliable difference in the latency of visual responses between the two subpopulations of neurons, with shorter latencies for cells showing a baseline shift effect (average difference across contrasts: 2.8 ms; $P = 0.02$, 2-way ANOVA; see Fig. 11A), suggesting a difference in general excitability, although other factors might well account for such differences (e.g., cells belonging to the 2 subpopulations might be located in different cortical layers, thus receiving different amount of direct top-down signals via feedback projections).

Further control analyses were performed to exclude the possibility that the baseline shift might be deterministically responsible for the poststimulus modulation by demonstrating that differences in attentional effects between the two subpopulations of cells (Fig. 10C) do not derive directly from spiking differences measured in the prestimulus phase. To this aim, for each attentional condition independently, we artificially sorted trials on the basis of prestimulus firing activity, dividing trials in which baseline activity was lower (low firing) or higher (high firing) than the median (median split). By doing this, for each attentional condition, we obtained two subsets of trials that were identical in terms of attentional condition but differed in terms of prestimulus activity, merely due to intertrial variability in neuronal firing (Fig. 11B). We then looked for any attention-like modulation of visually driven responses by artificially applying the previously used regression analysis (see Figs. 3, 4, and 10) to compare low-firing trials (potentially mimicking the "unattended" condition) vs. high-firing trials (potentially mimicking the "attended" condition) within each attentional condition. The temporal dynamics of attentional effects, as previously described (Figs. 3, 4, and 10), was not replicated (Fig. 11C), leading to the conclusion that even small changes in prestimulus activity generated by the allocation of attention in space are fundamentally different from those obtained by an arbitrary sorting of trials with different baseline activity within the same attentional condition. In other words,

attention-dependent baseline shifts should be viewed as a signature, and not as the direct cause, of the given attentional state and of the underlying network dynamics.

To sum up, in line with previous studies, we demonstrated a reliable modulation in the prestimulus epoch, confirming that macaque area V4 receives attentional feedback signals well before the stimulus appears. Interestingly, only about half of the cells in our population showed a reliable baseline shift; those cells are likely characterized by greater excitability, as confirmed by the tendency to show shorter latencies of visual response in the unattended condition (see above), and/or are located in different cortical layers, thus receiving different amount of direct top-down signals via feedback projections. In the absence of visual stimulation (i.e., for the 0% contrast stimulus), the baseline shift is maintained throughout the epoch of the trial we analyzed (Figs. 5 and 10). In the poststimulus epoch, a link emerges between the presence of a prestimulus modulation and the magnitude of the attentional modulation of responses to low-contrast stimuli; more specifically, prestimulus modulation contributes to the early contrast gain modulation. In addition, cells showing a reliable baseline shift seem to manifest stronger attentional modulation in terms of spike differences, across the whole poststimulus epoch (Fig. 10, *insets*). Critically, both cells showing a reliable baseline shift and cells without a prestimulus modulation show the delayed emergence of an attentional effect triggered by multiplicative mechanisms. The attentional effect measured in the intermediate epoch of visual processing, peaking ~150 ms after stimulus onset, is therefore independent from the manifestation of prestimulus activity and might instead be dependent on visual stimulation (Ekstrom et al. 2008; see DISCUSSION).

We acknowledge that a critical issue for the interpretation of the described dynamics of attentional effects might be related to the sustained nature of the stimuli in our paradigm. At least in principle, one might conjecture that prolonged stimulus availability in our paradigm (as a matter of fact, an indispensable feature for studying the time course of attentional effects) allows for online adjustments of attention. In fact, although the unpredictability of timing and contrast of both target and
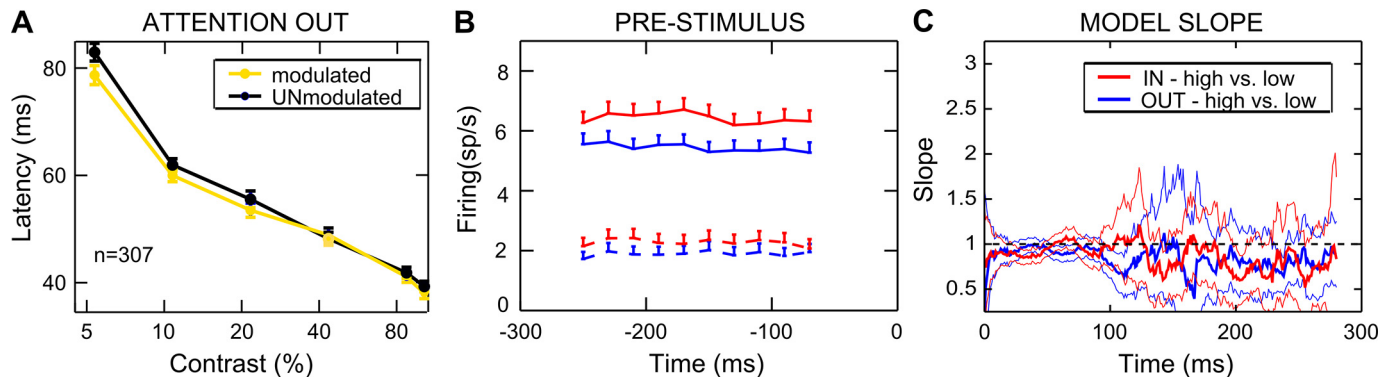

Fig. 11. Impact of prestimulus modulation on neuronal response latency and poststimulus attentional effects. A: averaged latency as a function of %contrast is plotted in the unattended condition, separately for the subpopulation of cells with (yellow) and without (black) a reliable baseline shift. Each point represents the average (mean ± SE) across neurons. B: time course of prestimulus modulation. Attentional modulation is calculated before stimulus onset in 100-ms windows, shifted by 25 ms, for 4 artificially sorted subpopulations of trials. Two subpopulations have been separated by selecting trials with high prestimulus firing (solid lines) and low prestimulus firing (dashed lines), separately for the unattended condition (blue lines) and attended condition (red lines). C: time course of the modulation effects exerted by the presence of high vs. low prestimulus baseline activity is shown separately for the attended (In; red line) and unattended (Out; blue line) conditions. The pattern of poststimulus activity in the low-firing condition is compared with the high-firing condition in a 20-ms window, shifted by 1 ms (see MATERIALS AND METHODS). Slope values of the regression lines calculated within each window are plotted as a function of time; thin lines mark 95% confidence intervals computed using the subsampling procedure (see MATERIALS AND METHODS). Note that despite the strong difference in firing patterns before stimulus onset (B), the time course of modulation does not replicate the poststimulus attentional effects shown in Figs. 3, 4, and 10.

distractor stimuli (see MATERIALS AND METHODS) makes predictive adjustments of attentional engagement highly unlikely, a reactive and somewhat delayed increase in attentional effort might follow the presentation of a low-contrast stimulus at the attended location inside the RF. Notwithstanding that the constant presence of mid/high-contrast distractors (outside the RF) renders variations in the attentional effort across trials rather unlikely (because attention must be focused at the RF location despite powerful distraction), thus weakening this potential concern, we believe that a more definite answer comes from a detailed analysis of the pattern of results. In fact, a boost of responses to low-contrast stimuli occurs in a very early phase after stimulus onset (Figs. 3–5, 10), a phase when attention is not affecting processing of high-contrast stimuli. Moreover, for cells with a reliable baseline shift, a strong attentional modulation of responses to low-contrast stimuli is maintained for the entire duration of stimulus processing (Fig. 10). Therefore, the evidence above appears to indicate that the temporal dynamics of attention gain mechanisms, as reported here, reflects some fundamental property of the circuits involved, rather than any fast-occurring, reactive adjustment of attentional effort, depending on the contrast of the stimulus.

DISCUSSION

We have presented a fine characterization of the temporal dynamics of attentional effects on visual responses in macaque area V4d, uncovering three crucial epochs of attentional modulation: an early stage dominated by contrast gain effects, a time-limited stimulus-dependent multiplicative gain modulation peaking at ~150 ms after stimulus onset, and a late stage characterized by the resurgence of contrast-gain. We also have disentangled the contribution of top-down prestimulus signals and stimulus-driven enhancement, embracing both the multiplicative and contrast gain stages. Finally, by characterizing attention-dependent modulation of single neuron CRFs, we have confirmed results described for the general population and described the contribution of different cell categories to the overall V4 attentional modulation.

Top-down signals and multiplicative enhancement of stimulus-driven responses. We considered the impact of top-down attention on the activity of V4 neurons during a relatively long epoch beginning before stimulus onset and extending to early-to-late phases of stimulus processing. Effects of attention on firing activity of visual neurons are thought to depend on attention-related feedback signals from higher cortical areas (Baluch and Itti 2011; Bisley and Goldberg 2010; Corbetta and Shulman 2002; Gottlieb 2007; Knudsen 2007; Noudoost et al. 2010), including the frontal cortex and, specifically, the frontal eye field (FEF; Gregoriou et al. 2009; Moore and Armstrong 2003; Moore and Fallah 2004). These signals are responsible for the prestimulus allocation of attention, as reflected by the baseline enhancement of cell firing in our data as well as in previous studies (Buffalo et al. 2010; Luck et al. 1997; McAdams and Maunsell 1999; Reynolds et al. 2000). The elevated baseline firing, in turn, may be part of the mechanism that confers the targeted V4 neurons increased sensitivity to visual stimulation (see *Top-down signals and increased contrast sensitivity*); in addition, the same top-down signals likely play a role in boosting coherent firing of neuronal populations (Chelazzi et al. 2011).

Recent findings demonstrated that the input from FEF to V4 is rather weak (and rapid) and that the majority of projections are of excitatory type (Anderson et al. 2011). Although compatible with the small but significant prestimulus modulation in V4, this weak input from FEF hardly explains the robust (and delayed) enhancement of stimulus-driven responses (Luck et al. 1997; McAdams and Maunsell 1999, 2000; Reynolds et al. 1999, 2000), unless forms of (time-consuming) signal amplification are hypothesized (Anderson et al. 2011). Interestingly, a previous fMRI study demonstrated in the macaque that bottom-up activation of early visual areas (including V4) is needed to enable strong top-down modulation from frontal areas (Ekstrom et al. 2008), suggesting stimulus dependence of multiplicative attentional effects. Our fine-grain temporal analysis of attentional effects adds critical new information to this issue. Specifically, we observed a stimulus-dependent response gain stage that was characterized by delayed emergence and affected all cells in the population, regardless of their permeability to top-down signals in the prestimulus epoch (Fig. 10). These data support the hypothesis that, after stimulus onset, the weak excitatory top-down input from higher order areas might be amplified by local recurrent circuits (Baluch and Itti 2011) and distributed to cells not immediately affected by the top-down signal. This amplification process likely requires substantial amount of time, which might well be reflected in the time needed for the multiplicative stage to be fully expressed in our data.

In terms of its functional meaning, the multiplicative stage likely corresponds to a decision stage of visual processing, when the representation of the attended stimulus fully dominates neural activity across distributed brain networks (Duncan 1998, 2006). In this phase, attention shields the relevant neuronal population from the inhibitory influence of competing neuronal populations (normalization pool), thus boosting its firing and enhancing signal transmission along the network. Accordingly, when two stimuli impinge on the RF of a neuron, directing attention to the preferred stimulus in the pair attenuates the suppressive effect of the ineffective stimulus (Reynolds and Chelazzi 2004; Reynolds and Desimone 2003; Sundberg et al. 2009). Of course, these effects are also likely mediated by changes in coherent activity within the critical population of neurons as well as across distant nodes within the network (Fries et al. 2008; Gregoriou et al. 2009, 2012; Schroeder and Lakatos 2009; Womelsdorf and Fries 2007).

Top-down signals and increased contrast sensitivity. In addition to a multiplicative rescaling of CRFs, attentional effects in our data manifest themselves as a contrast gain modulation in both an early and a late stage of visual processing. We submit that the nature and functional meaning of these two contrast gain stages is different.

The early contrast gain modulation appears to be strictly dependent on prestimulus modulation, being nearly absent in cells that do not show a reliable baseline shift (Fig. 10). Here, the increase in prestimulus activity with attention acts as a head start, rendering the critical neuronal population more prone to react to the stimulus, which may be in line with the small but reliable reduction in response latency with attention (Fig. 1F). In a similar vein, the baseline shift has been viewed as a facilitating prior of subsequent visual processing (Summerfield and de Lange 2014). Compatible with a subadditive mechanism, the beneficial influence of the preexisting baseline mod-

ulation becomes progressively weaker as the visual drive increases, thus selectively boosting weak feedforward input, while leaving the saturating portion of the CRFs largely unaffected. In keeping with our findings, microstimulation of the FEF was demonstrated to selectively enhance blood oxygen level-dependent (BOLD) activity in V4 (and other visual areas) in response to low-contrast stimuli while producing no effect for high-contrast stimuli (Ekstrom et al. 2009). Our results are also in agreement with what was recently described as an input baseline increase in neuronal activity that accounts for behavioral changes in perceived contrast, in line with an apparent contrast gain modulation of psychometric functions by attention (Cutrone et al. 2014).

The late contrast gain modulation is different from that observed in the early epoch (Fig. 10). First, the attentional effect is overall larger in terms of spike difference between the unattended and the attended condition. Second, the effect measured for low contrasts exceeds appreciably that measured for the null (zero contrast) stimulus, demonstrating a less direct dependence from the baseline shift. Moreover, although contrast gain modulation in this late epoch is stronger for those cells showing a reliable baseline shift, a similar pattern emerges also for cells not displaying such baseline effect. One possible account of the late contrast gain effect is that it represents an effective input gain modulation enhancing the contrast sensitivity of V4 neurons. It was recently demonstrated that attention increases efficacy of synaptic communication between the LGN and primary visual cortex (Briggs et al. 2013). A similar action might be hypothesized to enhance synaptic transmission of signals targeting area V4, for example, from V1–V2, or perhaps even directly boosting signal transmission along the topographically organized connections from the LGN to V4 (Gattass et al. 2014).

The proposed account of the late contrast gain effect is in agreement with what was recently put forward in the case of MT neurons, for which contrast-dependent modulations of spiking activity were observed and described as compatible with effective changes in the input strength into the area (Khayat et al. 2010; see also Martínez-Trujillo and Treue 2002). Moreover, it might also be interpreted in the framework of input gain models postulating selective and flexible attentional influences onto specific input signals, also based on their behavioral relevance (Ghose 2009; Ghose and Maunsell 2008). Although in the present study we tested the influence of attention on single stimuli within the RF of the recorded neurons, input gain effects might also be in place when multiple stimuli impinge onto the RF of the given neuron; in that case, selective boosting of input signals might increase the influence of the attended stimulus at the expenses of the unattended ones, thus contributing to effectively bias cross-stimulus competition (Chelazzi et al. 2011; Desimone and Duncan 1995; Reynolds and Chelazzi 2004). In the latter case, however, much more than when an isolated visual stimulus is considered, a most critical role would be played by mechanisms of lateral interactions and mutual inhibition, with the attentional effect likely acting prominently by modulating the strength of normalization (Reynolds and Heeger 2009), as also discussed in the previous paragraph.

Another potential account of the late contrast gain modulation might rely on a differential timing for the processing of low- vs. high-contrast stimuli, with the former requiring longer integration times. Following this logic, one could hypothesize that the entire attentional episodes, and in particular the multiplicative stage, are concluded earlier for relatively high- than low-contrast stimuli. One obvious implication is that this differential duration of attentional effects for low- vs. high-contrast stimuli might directly result in specific differences in the timing of behavioral responses, as illustrated in Fig. 1B. To push this further, one could predict a direct relationship between the duration of the multiplicative stage and the time required for reaching a decision. We tested this possibility in several ways, e.g., by selecting a subset of the data for which RTs were matched across contrasts, implying similar decision times across the selected trials (this was obtained by trimming the data separately for each single cell and each experimental condition based on single-trial RTs); specifically, for these data we predicted similar attentional effects across the whole contrast range during the last phase of visual processing. Instead, we fully replicated a late contrast gain modulation in the subset of trials with matched RTs. In sum, for specific contrasts, we did not find clear evidence of a direct link between the RT of the animal in the given trial and the strength of the attentional modulation, although a phenomenon of this kind might marginally contribute to the overall pattern of modulation.

In fact, there is no reason to view the two alternative explanations above as mutually exclusive. Rather, the late contrast gain modulation might result from a mixture of a pure input gain effect, selectively boosting the processing of weak feedforward input, and a pseudo-contrast gain deriving from the persistence of an attentional effect (from the multiplicative phase) for low contrasts due to longer integration times.

Links with previous studies. Previous studies supporting the contrast gain or the additive model (Martínez-Trujillo and Treue 2002; Reynolds et al. 1999; Thiele et al. 2009) typically averaged neuronal responses over long temporal windows and/or focused on late processing stages, thus either averaging across different gain phases or considering just a single (late) stage. Consistently, we found a late contrast gain modulation (Figs. 3 and 10) and an overall mixture of contrast gain and additive modulation when averaging over long time periods of the neuronal response. Analogously, our results are consistent with fMRI studies supporting contrast gain or additive models (Buracas and Boynton 2007; Li et al. 2008; Murray and He 2006). In fMRI experiments, the signal is in fact related to subthreshold and spiking activity averaged over long time periods and across neurons with different tuning properties (Hara et al. 2014). Importantly, our results are also coherent with an electrophysiological study by Williford and Maunsell (2006), reporting a prevalence of the response gain model in V4 neurons by averaging responses over a short time window (50–200 ms), which, according to our own results, mainly captures the multiplicative stage.

Our result might perhaps be reconciled within the normalization model framework proposed by Reynolds and Heeger (2009). In simple terms, the model posits that the excitatory stimulus drive impinging on a single neuron is normalized (divided) by the sum total drive across the neuronal population (suppressive drive). The effect of attention in the model is to multiply the excitatory drive for the neuron in a selective manner, before the impact of normalization. The model succeeds at predicting different effects of attention on neuronal firing (i.e., either a change in contrast gain or a multiplicative

scaling of the CRF) by taking into account the specific sensory conditions (e.g., the size of the RF stimulation) and the degree of attentional focusing. In line with this model, our findings suggest that different gain mechanisms should not be seen as alternative and mutually exclusive, but rather as reflecting different functional states of the underlying circuitry and/or different phases of processing. However, one of the model simplifications is that it does not consider the temporal evolution of attentional effects, nor does it consider the time needed to implement the described computations. Our data suggest that the inclusion of time among the crucial variables influencing both stimulus processing and attentional deployment might be highly beneficial (see also Smith et al. 2015). Moreover, the finding of a time-dependent impact of spatial attention on contrast coding calls for reinvestigations of the phenomenon in future behavioral experiments, with the aim of gaining a better understanding of how the described dynamical interactions may impact perception (e.g., by affecting perceptual stability) and behavior. For example, by varying the effective timing of visual stimulation through masking procedures, psychophysical evidence might be collected to directly reveal evolving functional states during the course of visual processing, with either contrast gain or response gain effects of attention to be measured depending on the given experimental manipulation (see also Smith et al. 2015). However, future studies should be carefully designed in consideration of the possibility that differences in task timing have themselves an impact on the underlying dynamics of attentional effects such that the system might be pushed to compress or dilate relevant phases of visual and attentional processing in accordance to task demands (for considerations on the issue of task timing, see also Khayat et al. 2010; Ling and Carrasco 2006).

Because we did not aim at testing the normalization model, our experimental approach did not comprise any specific manipulation of its critical variables; namely, both the stimulation and the attentional field size were kept constant across attentional conditions. Nonetheless, dynamic variations can be hypothesized during the unfolding of the trial. Specifically, according to our results, we conjecture that before stimulus onset, the attention field is already controlling neuronal responses in a broad region where the stimulus is likely to appear. Right after stimulus appearance, neuronal responses are characterized by a summation phase so that the stimulation field is initially small and possibly maximal at the RF center. The combination of a spatially extended attention field and a small visual stimulation might produce the early contrast gain effect. At a later stage, the stimulus is fully processed and the attention field is probably closely shaped around it; as a result, neuronal responses would be multiplicatively scaled. In other words, attention efficiently reduces the impact of the suppressive drive on neuronal responses during the intermediate phase of visual processing, where the stimulus representation is amplified. At the final stage, a resurgence of a contrast gain modulation might reflect a tendency for the attentional focus to relax in terms of spatial resolution (resulting again in a broad attention field) while remaining highly selective in the feature domain at the service of the discrimination task to be performed. To some extent, the described scenario might indirectly reflect a prevalent role of spatial attention in a prestimulus epoch and in an early-to-intermediate phase of visual processing, and a more relevant role of feature-based attention

in a later phase of the trial. Interestingly, somewhat related to our results, a different time course has been described for the effects of spatial and feature-based attention, with the former being progressively stronger after visual stimulation onset and the latter being rather constant throughout visual processing (Hayden and Gallant 2005). However, above and beyond potential differences in the intensity of attentional effects along the trial, what we describe here points to the notion that attention acts through different gain mechanisms evolving over time.

Attention and heterogeneous contrast coding. New to the field, in this study we separately analyzed the attentional effects for neurons with different coding properties, corroborating population findings. The shared temporal dynamics of attentional effects for neurons showing monotonic vs. selective CRFs supports the idea that attentional circuits are not specifically linked to the visual selectivity of V4 neurons, with all contrast categories contributing to general effects.

We previously demonstrated the existence of a consistent fraction of cells in macaque V4 displaying ban-pass tuning for luminance contrast and hypothesized that selective coding of contrast might be crucial for the attentive selection of specific contrast levels, by means of a feature-based mechanism that typically requires neural populations capable of selectively coding the to-be-attended feature (Sani et al. 2013). Presently, we add to this previous finding by showing for the first time that top-down control can boost this class of neurons.

Another intriguing result is the discovery of a nonnegligible fraction of cells for which attention to the RF changed the CRF shape. This phenomenon demonstrates that contrast coding is not a rigid property of the given neuron, in analogy to other neuronal properties (e.g., the spatial extent of RFs; see Ben Hamed et al. 2002; Tolias et al. 2001; Womelsdorf et al. 2006, 2008), and suggests a mechanism through which neurons might acquire the necessary selectivity to accommodate their properties to the nature of the current task. It remains to be demonstrated whether attention can selectively enhance specific subpopulations of V4 neurons, for example, the ones representing low-contrast stimuli in a task that requires the overriding of sensory-driven saliency on the basis of luminance contrast.

Overall, these data support the idea of V4 circuitry playing a key role in "selective extraction" of functional networks driven by both bottom-up or top-down signals (Roe et al. 2012). Accordingly, both the delayed emergence of contrast selectivity (Sani et al. 2013) and the precise temporal unfolding of attentional enhancement would result from the dynamical configuration of a feature extraction network. Although there is strong evidence that V4 might play such a crucial role, detailed temporal analysis of attentional modulation, as well as of coding strategies for contrast at the single-cell level, remain to be systematically explored in other visual areas.

GRANTS

DISCLOSURES

No conflicts of interest, financial or otherwise, are declared by the authors.

AUTHOR CONTRIBUTIONS

L.C. conceived and designed research; I.S. and E.S. performed experiments; I.S. and E.S. analyzed data; I.S., E.S., M.C.M., and L.C. interpreted results of experiments; I.S. and E.S. prepared figures; I.S. and E.S. drafted manuscript; I.S., E.S., M.C.M., and L.C. edited and revised manuscript; I.S., E.S., M.C.M., and L.C. approved final version of manuscript.

REFERENCES

Albrecht DG. Visual cortex neurons in monkey and cat: effect of contrast on the spatial and temporal phase transfer functions. *Vis Neurosci* 12: 1191–1210, 1995. doi:10.1017/S0952523800006817.

Albrecht DG, Farrar SB, Hamilton DB. Spatial contrast adaptation characteristics of neurones recorded in the cat's visual cortex. *J Physiol* 347: 713–739, 1984. doi:10.1113/jphysiol.1984.sp015092.

Albrecht DG, Hamilton DB. Striate cortex of monkey and cat: contrast response function. *J Neurophysiol* 48: 217–237, 1982.

Anderson JC, Kennedy H, Martin KA. Pathways of attention: synaptic relationships of frontal eye field to V4, lateral intraparietal cortex, and area 46 in macaque monkey. *J Neurosci* 31: 10872–10881, 2011. doi:10.1523/JNEUROSCI.0622-11.2011.

Astrand E, Ibos G, Duhamel JR, Ben Hamed S. Differential dynamics of spatial attention, position, and color coding within the parietofrontal network. *J Neurosci* 35: 3174–3189, 2015. doi:10.1523/JNEUROSCI.2370-14.2015.

Bair W, Cavanaugh JR, Movshon JA. Time course and time-distance relationships for surround suppression in macaque V1 neurons. *J Neurosci* 23: 7690–7701, 2003.

Baluch F, Itti L. Mechanisms of top-down attention. *Trends Neurosci* 34: 210–224, 2011. doi:10.1016/j.tins.2011.02.003.

Barlow HB, Blakemore C, Pettigrew JD. The neural mechanism of binocular depth discrimination. *J Physiol* 193: 327–342, 1967. doi:10.1113/jphysiol.1967.sp008360.

Ben Hamed S, Duhamel JR, Bremmer F, Graf W. Visual receptive field modulation in the lateral intraparietal area during attentive fixation and free gaze. *Cereb Cortex* 12: 234–245, 2002. doi:10.1093/cercor/12.3.234.

Bisley JW, Goldberg ME. Attention, intention, and priority in the parietal lobe. *Annu Rev Neurosci* 33: 1–21, 2010. doi:10.1146/annurev-neuro-060909-152823.

Briggs F, Mangun GR, Usrey WM. Attention enhances synaptic efficacy and the signal-to-noise ratio in neural circuits. *Nature* 499: 476–480, 2013. doi:10.1038/nature12276.

Buffalo EA, Fries P, Landman R, Liang H, Desimone R. A backward progression of attentional effects in the ventral stream. *Proc Natl Acad Sci USA* 107: 361–365, 2010. doi:10.1073/pnas.0907658106.

Buracas GT, Boynton GM. The effect of spatial attention on contrast response functions in human visual cortex. *J Neurosci* 27: 93–97, 2007. doi:10.1523/JNEUROSCI.3162-06.2007.

Chelazzi L, Della Libera C, Sani I, Santandrea E. Neural basis of visual selective attention. *Wiley Interdiscip Rev Cogn Sci* 2: 392–407, 2011. doi:10.1002/wcs.117.

Corbetta M, Shulman GL. Control of goal-directed and stimulus-driven attention in the brain. *Nat Rev Neurosci* 3: 201–215, 2002. doi:10.1038/nrn755.

Cutrone EK, Heeger DJ, Carrasco M. Attention enhances contrast appearance via increased input baseline of neural responses. *J Vis* 14: 16, 2014. doi:10.1167/14.14.16.

Desimone R, Duncan J. Neural mechanisms of selective visual attention. *Annu Rev Neurosci* 18: 222, 1995. doi:10.1146/annurev.ne.18.030195.001205.

DiCiccio TJ, Efron B. Bootstrap confidence intervals. *Stat Sci* 11: 189–228, 1996. doi:10.1214/ss/1032280214.

Duncan J. Converging levels of analysis in the cognitive neuroscience of visual attention. *Philos Trans R Soc Lond B Biol Sci* 353: 1307–1317, 1998. doi:10.1098/rstb.1998.0285.

Duncan J. EPS Mid-Career Award 2004: brain mechanisms of attention. *Q J Exp Psychol (Hove)* 59: 2–27, 2006. doi:10.1080/17470210500260674.

Ekstrom LB, Roelfsema PR, Arsenault JT, Bonmassar G, Vanduffel W. Bottom-up dependent gating of frontal signals in early visual cortex. *Science* 321: 414–417, 2008. doi:10.1126/science.1153276.

Ekstrom LB, Roelfsema PR, Arsenault JT, Kolster H, Vanduffel W. Modulation of the contrast response function by electrical microstimulation of the macaque frontal eye field. *J Neurosci* 29: 10683–10694, 2009. doi:10.1523/JNEUROSCI.0673-09.2009.

Fries P, Womelsdorf T, Oostenveld R, Desimone R. The effects of visual stimulation and selective visual attention on rhythmic neuronal synchronization in macaque area V4. *J Neurosci* 28: 4823–4835, 2008. doi:10.1523/JNEUROSCI.4499-07.2008.

Gattass R, Galkin TW, Desimone R, Ungerleider LG. Subcortical connections of area V4 in the macaque. *J Comp Neurol* 522: 1941–1965, 2014. doi:10.1002/cne.23513.

Gawne TJ, Kjaer TW, Richmond BJ. Latency: another potential code for feature binding in striate cortex. *J Neurophysiol* 76: 1356–1360, 1996.

Ghose GM. Attentional modulation of visual responses by flexible input gain. *J Neurophysiol* 101: 2089–2106, 2009. doi:10.1152/jn.90654.2008.

Ghose GM, Maunsell JH. Spatial summation can explain the attentional modulation of neuronal responses to multiple stimuli in area V4. *J Neurosci* 28: 5115–5126, 2008. doi:10.1523/JNEUROSCI.0138-08.2008.

Gottlieb J. From thought to action: the parietal cortex as a bridge between perception, action, and cognition. *Neuron* 53: 9–16, 2007. doi:10.1016/j.neuron.2006.12.009.

Gregoriou GG, Gotts SJ, Desimone R. Cell-type-specific synchronization of neural activity in FEF with V4 during attention. *Neuron* 73: 581–594, 2012. doi:10.1016/j.neuron.2011.12.019.

Gregoriou GG, Gotts SJ, Zhou H, Desimone R. High-frequency, long-range coupling between prefrontal and visual cortex during attention. *Science* 324: 1207–1210, 2009. doi:10.1126/science.1171402.

Hara Y, Pestilli F, Gardner JL. Differing effects of attention in single-units and populations are well predicted by heterogeneous tuning and the normalization model of attention. *Front Comput Neurosci* 8: 12, 2014. doi:10.3389/fncom.2014.00012.

Hayden BY, Gallant JL. Time course of attention reveals different mechanisms for spatial and feature-based attention in area V4. *Neuron* 47: 643, 2005. doi:10.1016/j.neuron.2005.07.020.

Henry CA, Joshi S, Xing D, Shapley RM, Hawken MJ. Functional characterization of the extraclassical receptive field in macaque V1: contrast, orientation, and temporal dynamics. *J Neurosci* 33: 6230–6242, 2013. doi:10.1523/JNEUROSCI.4155-12.2013.

Ibos G, Duhamel JR, Ben Hamed S. A functional hierarchy within the parietofrontal network in stimulus selection and attention control. *J Neurosci* 33: 8359–8369, 2013. doi:10.1523/JNEUROSCI.4058-12.2013.

Jeurissen D, Self MW, Roelfsema PR. Surface reconstruction, figure-ground modulation, and border-ownership. *Cogn Neurosci* 4: 50–52, 2013. doi:10.1080/17588928.2012.748025.

Kastner S, Pinsk MA, De Weerd P, Desimone R, Ungerleider LG. Increased activity in human visual cortex during directed attention in the absence of visual stimulation. *Neuron* 22: 751–761, 1999. doi:10.1016/S0896-6273(00)80734-5.

Khayat PS, Niebergall R, Martinez-Trujillo JC. Attention differentially modulates similar neuronal responses evoked by varying contrast and direction stimuli in area MT. *J Neurosci* 30: 2188–2197, 2010. doi:10.1523/JNEUROSCI.5314-09.2010.

Knudsen EI. Fundamental components of attention. *Annu Rev Neurosci* 30: 57–78, 2007. doi:10.1146/annurev.neuro.30.051606.094256.

Kogo N, Wagemans J. The emergent property of border-ownership and the perception of illusory surfaces in a dynamic hierarchical system. *Cogn Neurosci* 4: 54–61, 2013. doi:10.1080/17588928.2012.754750.

Layton OW, Mingolla E, Yazdanbakhsh A. Dynamic coding of border-ownership in visual cortex. *J Vis* 12: 8, 2012. doi:10.1167/12.13.8.

Ledgeway T, Zhan C, Johnson AP, Song Y, Baker CL Jr. The direction-selective contrast response of area 18 neurons is different for first- and second-order motion. *Vis Neurosci* 22: 99, 2005. doi:10.1017/S0952523805221120.

Lee J, Maunsell JH. A normalization model of attentional modulation of single unit responses. *PLoS One* 4: e4651, 2009. doi:10.1371/journal.pone.0004651.

Lee J, Maunsell JH. The effect of attention on neuronal responses to high and low contrast stimuli. *J Neurophysiol* 104: 971, 2010. doi:10.1152/jn.01019.2009.

Lee J, Williford T, Maunsell JH. Spatial attention and the latency of neuronal responses in macaque area V4. *J Neurosci* 27: 9632–9637, 2007. doi:10.1523/JNEUROSCI.2734-07.2007.

Li X, Lu ZL, Tjan BS, Dosher BA, Chu W. Blood oxygenation level-dependent contrast response functions identify mechanisms of covert attention in early visual areas. *Proc Natl Acad Sci USA* 105: 6202–6207, 2008. doi:10.1073/pnas.0801390105.

Ling S, Carrasco M. Sustained and transient covert attention enhance the signal via different contrast response functions. *Vision Res* 46: 1210–1220, 2006. doi:10.1016/j.visres.2005.05.008.

Luck SJ, Chelazzi L, Hillyard SA, Desimone R. Neural mechanisms of spatial selective attention in areas V1, V2, and V4 of macaque visual cortex. *J Neurophysiol* 77: 24–42, 1997.

Martínez-Trujillo J, Treue S. Attentional modulation strength in cortical area MT depends on stimulus contrast. *Neuron* 35: 365–370, 2002. doi:10.1016/S0896-6273(02)00778-X.

McAdams CJ, Maunsell JH. Effects of attention on orientation-tuning functions of single neurons in macaque cortical area V4. *J Neurosci* 19: 431–441, 1999.

McAdams CJ, Maunsell JH. Attention to both space and feature modulates neuronal responses in macaque area V4. *J Neurophysiol* 83: 1751–1755, 2000.

Mirabella G, Bertini G, Samengo I, Kilavik BE, Frilli D, Della Libera C, Chelazzi L. Neurons in area V4 of the macaque translate attended visual features into behaviorally relevant categories. *Neuron* 54: 303–318, 2007. doi:10.1016/j.neuron.2007.04.007.

Moore T, Armstrong KM. Selective gating of visual signals by microstimulation of frontal cortex. *Nature* 421: 370–373, 2003. doi:10.1038/nature01341.

Moore T, Fallah M. Microstimulation of the frontal eye field and its effects on covert spatial attention. *J Neurophysiol* 91: 152–162, 2004. doi:10.1152/jn.00741.2002.

Motter BC. Central V4 receptive fields are scaled by the V1 cortical magnification and correspond to a constant-sized sampling of the V1 surface. *J Neurosci* 29: 5749–5757, 2009. doi:10.1523/JNEUROSCI.4496-08.2009.

Murray SO, He S. Contrast invariance in the human lateral occipital complex depends on attention. *Curr Biol* 16: 606–611, 2006. doi:10.1016/j.cub.2006.02.019.

Noudoost B, Chang MH, Steinmetz NA, Moore T. Top-down control of visual attention. *Curr Opin Neurobiol* 20: 183–190, 2010. doi:10.1016/j.conb.2010.02.003.

Peirce JW. The potential importance of saturating and supersaturating contrast response functions in visual cortex. *J Vis* 7: 13, 2007. doi:10.1167/7.6.13.

Politis DN, Romano JP. Large sample confidence regions based on subsamples under minimal assumptions. *Ann Stat* 22: 2050, 1994. doi:10.1214/aos/1176325770.

Ress D, Backus BT, Heeger DJ. Activity in primary visual cortex predicts performance in a visual detection task. *Nat Neurosci* 3: 940–945, 2000. doi:10.1038/78856.

Reynolds JH, Chelazzi L. Attentional modulation of visual processing. *Annu Rev Neurosci* 27: 611–647, 2004. doi:10.1146/annurev.neuro.26.041002.131039.

Reynolds JH, Chelazzi L, Desimone R. Competitive mechanisms subserve attention in macaque areas V2 and V4. *J Neurosci* 19: 1736–1753, 1999.

Reynolds JH, Desimone R. Interacting roles of attention and visual salience in V4. *Neuron* 37: 853–863, 2003. doi:10.1016/S0896-6273(03)00097-7.

Reynolds JH, Heeger DJ. The normalization model of attention. *Neuron* 61: 168–185, 2009. doi:10.1016/j.neuron.2009.01.002.

Reynolds JH, Pasternak T, Desimone R. Attention increases sensitivity of V4 neurons. *Neuron* 26: 703–714, 2000. doi:10.1016/S0896-6273(00)81206-4.

Ringach DL, Hawken MJ, Shapley R. Dynamics of orientation tuning in macaque primary visual cortex. *Nature* 387: 281–284, 1997. doi:10.1038/387281a0.

Roe AW, Chelazzi L, Connor CE, Conway BR, Fujita I, Gallant JL, Lu H, Vanduffel W. Toward a unified theory of visual area V4. *Neuron* 74: 12–29, 2012. doi:10.1016/j.neuron.2012.03.011.

Sani I, Santandrea E, Golzar A, Morrone MC, Chelazzi L. Selective tuning for contrast in macaque area V4. *J Neurosci* 33: 18583–18596, 2013. doi:10.1523/JNEUROSCI.3465-13.2013.

Schroeder CE, Lakatos P. Low-frequency neuronal oscillations as instruments of sensory selection. *Trends Neurosci* 32: 9–18, 2009. doi:10.1016/j.tins.2008.09.012.

Shapley R, Hawken M, Ringach DL. Dynamics of orientation selectivity in the primary visual cortex and the importance of cortical inhibition. *Neuron* 38: 689–699, 2003. doi:10.1016/S0896-6273(03)00332-5.

Smith PL, Sewell DK, Lilburn SD. From shunting inhibition to dynamic normalization: Attentional selection and decision-making in brief visual displays. *Vision Res* 116: 219–240, 2015. doi:10.1016/j.visres.2014.11.001.

Sripati AP, Johnson KO. Dynamic gain changes during attentional modulation. *Neural Comput* 18: 1847–1867, 2006. doi:10.1162/neco.2006.18.8.1847.

Sugihara T, Qiu FT, von der Heydt R. The speed of context integration in the visual cortex. *J Neurophysiol* 106: 374–385, 2011. doi:10.1152/jn.00928.2010.

Summerfield C, de Lange FP. Expectation in perceptual decision making: neural and computational mechanisms. *Nat Rev Neurosci* 15: 745–756, 2014. doi:10.1038/nrn3838.

Sundberg KA, Mitchell JF, Gawne TJ, Reynolds JH. Attention influences single unit and local field potential response latencies in visual cortical area V4. *J Neurosci* 32: 16040–16050, 2012. doi:10.1523/JNEUROSCI.0489-12.2012.

Sundberg KA, Mitchell JF, Reynolds JH. Spatial attention modulates center-surround interactions in macaque visual area v4. *Neuron* 61: 952–963, 2009. doi:10.1016/j.neuron.2009.02.023.

Sylvester CM, Shulman GL, Jack AI, Corbetta M. Anticipatory and stimulus-evoked blood oxygenation level-dependent modulations related to spatial attention reflect a common additive signal. *J Neurosci* 29: 10671–10682, 2009. doi:10.1523/JNEUROSCI.1141-09.2009.

Theeuwes J, Olivers CN, Belopolsky A. Stimulus-driven capture and contingent capture. *Wiley Interdiscip Rev Cogn Sci* 1: 872–881, 2010. doi:10.1002/wcs.83.

Thiele A, Pooresmaeili A, Delicato LS, Herrero JL, Roelfsema PR. Additive effects of attention and stimulus contrast in primary visual cortex. *Cereb Cortex* 19: 2970–2981, 2009. doi:10.1093/cercor/bhp070.

Tolias AS, Moore T, Smirnakis SM, Tehovnik EJ, Siapas AG, Schiller PH. Eye movements modulate visual receptive fields of V4 neurons. *Neuron* 29: 757–767, 2001. doi:10.1016/S0896-6273(01)00250-1.

Williford T, Maunsell JH. Effects of spatial attention on contrast response functions in macaque area V4. *J Neurophysiol* 96: 40–54, 2006. doi:10.1152/jn.01207.2005.

Womelsdorf T, Anton-Erxleben K, Pieper F, Treue S. Dynamic shifts of visual receptive fields in cortical area MT by spatial attention. *Nat Neurosci* 9: 1156–1160, 2006. doi:10.1038/nn1748.

Womelsdorf T, Anton-Erxleben K, Treue S. Receptive field shift and shrinkage in macaque middle temporal area through attentional gain modulation. *J Neurosci* 28: 8934–8944, 2008. doi:10.1523/JNEUROSCI.4030-07.2008.

Womelsdorf T, Fries P. The role of neuronal synchronization in selective attention. *Curr Opin Neurobiol* 17: 154–160, 2007. doi:10.1016/j.conb.2007.02.002.

Zhou H, Friedman HS, von der Heydt R. Coding of border ownership in monkey visual cortex. *J Neurosci* 20: 6594–6611, 2000.